

ISTANBUL TECHNICAL UNIVERSITY ★ GRADUATE SCHOOL OF SCIENCE
ENGINEERING AND TECHNOLOGY

**THEORETICAL AND EXPERIMENTAL VIBRATION ANALYSIS OF
STEERING WHEEL OF A HEAVY COMMERCIAL VEHICLE**

M.Sc. THESIS

Begüm DEREBAŞ

Department of Mechanical Engineering

Solid Mechanics Programme

MAY 2014

ISTANBUL TECHNICAL UNIVERSITY ★ GRADUATE SCHOOL OF SCIENCE
ENGINEERING AND TECHNOLOGY

**THEORETICAL AND EXPERIMENTAL VIBRATION ANALYSIS OF
STEERING WHEEL OF A HEAVY COMMERCIAL VEHICLE**

M.Sc. THESIS

Begüm DEREBAŞ
(503101511)

Department of Mechanical Engineering

Solid Mechanics Programme

Thesis Advisor: Öğr. Gör. Dr. Adil YÜCEL

MAY 2014

İSTANBUL TEKNİK ÜNİVERSİTESİ ★ FEN BİLİMLERİ ENSTİTÜSÜ

**BİR AĞIR TİCARİ VASITADA DİREKSİYON TİTREŞİMİNİN TEORİK VE
DENEYSEL İNCELEMESİ**

YÜKSEK LİSANS TEZİ

**Begüm DEREBAY
(503101511)**

Makina Mühendisliği Anabilim Dalı

Katı Cisimlerin Mekaniği Programı

Tez Danışmanı: Öğr. Gör. Dr. Adil YÜCEL

MAYIS 2014

Begüm Derebay, a **M.Sc.** student of ITU **Graduate School of Science Engineering and Technology** student ID **503101511**, successfully defended the **thesis** entitled “**Theoretical And Experimental Vibration Analysis of Steering Wheel of a Heavy Commercial Vehicle**” which she prepared after fulfilling the requirements specified in the associated legislations, before the jury whose signatures are below.

Thesis Advisor : **Öğr. Gör. Dr. Adil YÜCEL**

Istanbul Technical University

Jury Members : **Prof.Dr. M. Alaittin ARPACI**

Istanbul Technical University

Prof. Dr. Rahmi GÜÇLÜ

Yildiz Technical University

Date of Submission : 05 May 2014

Date of Defense : 05 June 2014

To my family,

FOREWORD

I would like to thank Dr. Adil YÜCEL and Prof. M. Alaittin ARPACI for their supervision, guidance and expertise during this work. I would like especially to thank FORD OTOSAN A.Ş. for their support in performing the experiments summarised in this paper. And finally the greatest thanks to my parents for their moral support.

May 2014

Begüm Derebay
(Mechanical Engineer)

TABLE OF CONTENTS

	<u>Page</u>
FOREWORD	ix
TABLE OF CONTENTS	xi
ABBREVIATIONS	xiii
LIST OF TABLES	xv
LIST OF FIGURES	xvii
SUMMARY	xix
ÖZET	xxi
1. INTRODUCTION	1
1.1 Purpose of Thesis	1
1.2 Literature Review	2
1.3 Hypothesis	9
2. SOURCES OF STEERING WHEEL VIBRATION	10
2.1 Steering System Decomposition in Heavy Commercial Vehicles	10
2.2 Sources of Steering Wheel Vibration of Heavy Commercial Vehicles	14
2.1.1 Brake judder (Shudder)	16
2.1.2 Shimmy and nibble.....	18
2.1.3 Shake and idle shake	21
4. BACKGROUND OF ROOT CAUSE INVESTIGATION OF HXXX STEERING WHEEL VIBRATION	22
5. EXPERIMENTAL MODAL ANALYSIS OF HXXX STEERING WHEEL	28
5.1 Test Instrumentation, Preparation and Setup.....	28
5.2 Modal Test of Steering Wheel and Column on Vehicle.....	32
5.3 Modal Test of Steering Wheel Free-Free Condition	35
5.4 Results of the Experimental Modal Analysis	36
5. FINITE ELEMENT MODAL ANALYSIS OF HXXX STEERING WHEEL AND COLUMN	38
5.1 Finite Element Model of Trimmed Body	38
5.2 Finite Element Model of the Steering Wheel	41
5.3 Results of the Finite Element Analysis	42
5.3.1 Finite element analysis of the trimmed body	43
5.3.2 Finite element analysis of steering wheel in free-free condition	46
6. CONCLUSIONS AND RECOMMENDATIONS	49
REFERENCES	50
CURRICULUM VITAE	53

ABBREVIATIONS

CAE	: Computer Aided Engineering
DOF	: Degree of Freedom
DTV	: Disc Thickness Variation
FEA	: Finite Element Analysis
FEM	: Finite Element Method
FRF	: Frequency Response Function
NVH	: Noise, Vibration Harshness
ODS	: Operating Deflection Shape
RSS	: Root Sum Square
SRO	: Disc Sideface Runout
SW	: Steering Wheel
TEI	: Thermoelastic Instability
WOT	: Wide Open Throttle

LIST OF TABLES

	<u>Page</u>
Table 3.1 : Comparison of the initial steering wheel vibration levels of vehicles A and B at idle.	23
Table 3.2 : Engine active side bracket vibration RSS measurements.	23
Table 3.3 : Steering wheel vibration velocity (mm/s).	24
Table 3.4 : Comparison of steering wheel vibration adjustment mechanism locked and unlocked.	25
Table 3.5 : HXXX Steering column modes.	26
Table 4.1 : Specification and calibration chart of the accelerometers.	30
Table 4.2 : Specifications of the impact hammers used for the modal test.	31
Table 4.3 : Steering wheel and column modes.	37
Table 4.4 : Modes directions of the steering wheel and column.	37
Table 5.1 : Steering wheel and column modes according to trimmed body CAE results.	45
Table 5.2 : Natural frequencies of HXXX steering wheel in free – free condition. .	47
Table 5.3 : Comparison of experimental and finite element modal analysis	48

LIST OF FIGURES

	<u>Page</u>
Figure 1.1 : FE model correlation process.	9
Figure 2.1 : HXXX CAE model.....	10
Figure 2.2 : Steering system components of a truck.	11
Figure 2.3 : HXXX axle beam steering and suspension system.	13
Figure 2.4 : Three axes of vibration measured on a steering a wheel.....	14
Figure 2.5 : Sketch of the main suspension systems and vibration sources of a heavy truck.....	15
Figure 2.6 : Uneven thermal distributions on disc brake.	17
Figure 2.7 : Disc brake thickness variation.....	18
Figure 2.8 : Steering wheel vibration due to road roughness.	19
Figure 2.9 : Transfer path of steering shimmy and brake judder.....	20
Figure 2.10 : Steering wheel shimmy and nibble.....	20
Figure 2.11 : Steering wheel shake.	21
Figure 2.12 : Steering shimmy and shake.	21
Figure 3.1 : Accelerometer placement on engine active side bracket.....	23
Figure 3.2 : Directions of first and second mode of the steering column.	26
Figure 3.3 : Introduced steering column lower side bolt connections.	27
Figure 3.4 : Steering column – cross car beam connection reinforcements added (above) instead of the L-shaped bracket (bottom).	27
Figure 4.1 : Test setup plan for steering wheel modal testing.	29
Figure 4.2 : Brüel&Kjær triaxial accelerometer.	29
Figure 4.3 : Impact hammer used for first test (hammer #1) which was performed on HXXX steering wheel as attached to cab.....	31
Figure 4.4 : Impact hammer used for the second test (hammer #2).....	31
Figure 4.5 : Measurement and data processing equipment.....	32
Figure 4.6 : HXXX steering wheel on vehicle.....	33
Figure 4.7 : Accelerometer locations on steering wheel.	33
Figure 4.8 : Accelerometers #9 and #10 located on steering column.	34
Figure 4.9 : Accelerometer positioning on the steering wheel, Point-1 (excitation point).	34
Figure 4.10 : Impact and measurement points on the steering wheel.	35
Figure 4.11 : Example of frequency response function (accelerance).....	36
Figure 4.12 : Coherence function diagram.....	36
Figure 4.13 : FRF stabilization diagram.	37
Figure 5.1 : Quality criteria definitions of shell and solid mesh.....	39
Figure 5.2 : Finite element model of the cab.	40
Figure 5.3 : Display model.....	40
Figure 5.4 :Steering wheel assembly finite element model.	41
Figure 5.5 : Steering wheel solid mesh (left) and shell mesh (right).	42

Figure 5.6 : Steering wheel insert model (left), steering wheel single point constraint point (right).	42
Figure 5.7 : Mode shapes of steering wheel and column without proposed bolts.	43
Figure 5.8 : Trimmed body frequency – mode diagram.	44
Figure 5.9 : Nodes selected to obtain the modal frequencies.....	45
Figure 5.10 : Steering wheel frequency – mode diagram.	46
Figure 5.11 : Mode shapes of the steering wheel.....	47
Figure 5.12 : Previous steering wheel FE model.	48

THEORETICAL AND EXPERIMENTAL VIBRATION ANALYSIS OF STEERING WHEEL OF A HEAVY COMMERCIAL VEHICLE

SUMMARY

Steering wheel vibration is one of the biggest noise, vibration and harshness (NVH) problems in automotive engineering since it affects driver's comfort directly. It has been a serious problem especially for long distance drivers such as heavy commercial vehicle drivers due to long exposure periods. The purpose of this thesis is to investigate the root cause of the steering wheel vibration of a particular heavy commercial vehicle model, program code named HXXX, and validation of the CAE model of the steering wheel and trimmed body by the help of the results of experimental modal analysis performed on the steering wheel and column. Once correlation between finite element analysis and test results established, several design change iterations and their effects on the changing dynamic behaviour of the steering system can be observed without performing tests.

This thesis first introduces a survey of the literature on sources of steering wheel vibration, experimental and analysis methods applied to investigate the sources of the vibration and optimization and improvement of steering wheel vibration in passenger cars or trucks. On the basis of the literature survey, improvement recommendations can be made which might be implemented with the new coming program in order to reduce the steering wheel vibration of mentioned particular truck in the further stages of the program.

The second chapter presents the components of this particular heavy commercial truck which have an effect on steering wheel vibration and examines most common sources of steering wheel vibration and concentrates on major contributing factors of the vibration.

In the third chapter, determination process of root cause of the HXXX steering wheel vibration will be discussed in detail.

In the fourth chapter modal analysis and hammer impact test set-up and results will be illustrated. Test methodology will be presented in depth. Suggestions which takes place in literature will be implemented in the test process to get more accurate results.

In the fifth chapter finite element modelling and analysis results will be presented and discussed. Finite element model consists of the whole cab of the truck including body-in-prime, exterior and interior trim components. Cabin suspension, chassis frame, and chassis related parts are not incorporated in the model.

In the sixth chapter, comparison of the test results with finite element analysis results will be presented and design improvement recommendations for reduction of the steering wheel vibration which can be applicable with the new-coming vehicle program will be discussed.

AĞIR TİCARİ BİR TAŞITTA DİREKSİYON TİTREŞİMİNİN TEORİK VE DENEYSEL OLARAK ANALİZİ

ÖZET

Bir araçta gözlemlenen titreşimlerin sebebi motor, aktarma organları, lastiğin yola temas yüzeyi, yol yüzeyi, fren ve rüzgar gibi birçok sayıda etken olabilmektedir. Direksiyon titreşimi, sürücünün direksiyon simidi ile doğrudan ilişkisi göz önünde bulundurulduğunda ve araç kullanım süresi boyunca aralıksız temas edilmesi sebebiyle otomotiv mühendisliğinin üzerinde çalıştığı en büyük titreşim problemlerden biri olmuştur. Özellikle ağır ticari vasıtalarda, uzun süreli araç kullanımından dolayı direksiyon titreşimi sürücü konforunu doğrudan etkileyen bir titreşim sorunu olmaktadır. Bu çalışmada taşıtlarda direksiyon titreşimine neden olan kaynak ve transfer yollarının anlaşılmasının yanı sıra HXXX kodlu bir ağır ticari vasıtada geliştirme aşamasında tespit edilen direksiyon titreşiminin nedenlerinin araştırılması için yapılan testler ile sonlu eleman analizi modellemesinin korelasyonuna ait çalışmalara yer verilecektir.

Tezin inceleme konusu direksiyon titreşim kaynaklarının incelenmesi, HXXX direksiyon titreşimi temel neden analizi, dizayn modifikasyonları sonrası HXXX direksiyon simit ve kolon modlarının tespiti, direksiyon model iyileştirmesi ve korelasyonu ve test ve analiz sonuçlarıdır. Çalışmada sonlu eleman analizi ve deneysel model analiz metodları kullanılmıştır. Çalışmanın amacı HXXX direksiyon titreşiminin azaltılması (direksiyon kolon birinci modunun mümkün olduğunca 35 Hz ve üzeri mertebelere çıkarılması) ve direksiyon modelinin doğrulamasıdır.

Birinci bölümünde direksiyon titreşimi kök neden araştırması, direksiyon titreşiminin deneysel ve teorik yöntemlerle incelenmesi ve direksiyon titreşiminin azaltılması için yapılan literatür çalışmaları kısaca sunulmuştur. Literatürde direksiyon titreşimi konusunda birçok sayıda makale yayınlanmış olup, direksiyon simit ve kolon dinamik davranışlarının tespiti amacıyla pek çok deneysel ve teorik çalışma yapılmıştır. Direksiyon titreşimine sebep olan titreşim kaynakları ve direksiyon titreşimini azaltmaya yönelik optimizasyon çalışmalarına da literatür araştırmasında yer verilmiştir. Ağır ticari vasıtalarda süspansiyon sistemi, lastik ve jant sistemi, motor ve aktarma organları, fren sistemi ve yol (dış kaynak) titreşimin kaynakları arasındadır. Fren kaynaklı titreşimler, fren diski yüzeyindeki süreksizlikler (disk kalınlık varyasyonu, disk yüzeyinde aşınma, termoelastik dengesizlik), kampanalı fren deformasyonu ya da hatalı montaj nedeniyle ortaya çıkabilen direksiyonda dikey doğrultuda ya da ileri geri titreşimler ile farkedilebilen titreşimlerdir. Yol kaynaklı titreşimler (yol yüzeyi düzensizlikleri) ile lastik ve jant kaynaklı titreşimler (dengesiz lastik / jant, lastik düzgünsüzlüğü) orta hızlarda meydana gelen rotasyonel titreşimlerdir. Güç aktarma organları kaynaklı titreşimler (motor rölanti titreşimleri, dengesiz güç aktarma organları, tork dalgalanması) daha çok 10-30 Hz aralığında ortaya çıkan dikey ya da titreşimler meydana getirir.

İkinci bölümde ağır ticari taşıt direksiyon sistemi komponentleri tanıtılmış, araçlarda görülen direksiyon titreşim tiplerine göre titreşimde rolü olabilecek kaynaklar ve transfer yolları hakkında bilgi verilmiştir. Direksiyonda gözlemlenen titreşimin doğrultusuna ve frekans aralığına göre titreşimin kaynağı hakkında fikir sahibi olabilmek ve kök neden araştırmasını bu doğrultuda yapabilmek amaçlanmıştır. Yol pürüzlülüğü, lastik ve jant düzgünsüzlükleri ve dengesizlikleri, disk fren sistemindeki disk kalınlık varyasyonu, disk yüzeyinin aşınması, motor rölanti frekansının direksiyon kolon frekansı ile çakışması gibi bir araçta direksiyon titreşimine neden olabilecek kaynaklar incelenmiştir.

Üçüncü bölümde HXXX araç programı geliştirme aşamasında tespit edilen direksiyon titreşiminin nedenleri ve ortadan kaldırmaya yönelik dizayn değişiklik önerileri sunulmuştur. Direksiyon titreşiminin kök neden analizi, en kötü (A) ve en iyi (B) olarak belirlenen iki prototip araç üzerinde testler gerçekleştirilerek tespit edilmiştir. Kök neden analizinde izlenen adımlar, titreşimin kaynağı olarak motor titreşim seviyesinin ölçülmesi, mod izolasyonunun tespiti için güç aktarma organları rijit yuvarlanma modunun ölçülmesi, transfer yolu olarak motor takoz etkisinin araştırılması, transfer yolu olarak direksiyon ayar mekanizması ve kolon – ön konsol bağlantısının etkisinin araştırılması olarak sıralanabilir. En yüksek ve en düşük seviyede direksiyon titreşimine sahip iki prototip araçta motor takozlarının ve direksiyon sisteminin titreşim seviyeleri ölçülmüştür. Testler motor rölantideyken yapılmıştır. 2 adet 3D ivmeölçer arka motor takozlarına ve 1 adet 3D ivmeölçer direksiyona bağlanarak ölçümler alınmıştır. Yapılan testler sonucunda titreşimin kaynağı motor takozlarının yüksek rijitlikte olması ve motor yuvarlanma modu ile direksiyon kolonunun doğal frekanslarının çakışması olarak belirlenmiştir. Direksiyon kilit mekanizmasının titreşimin transferinde oynadığı rol tespit edilmiştir. Yapılan kök neden araştırması sonucunda motor rölanti devrinin değiştirilmesi, motor takozlarının rijitliğinin azaltılması ve direksiyon kolon modunun artırılması için çeşitli dizayn değişiklikleri önerilmiştir. Programın ileriki aşamalarında uygulamaya koyulan dizayn değişiklikleri gösterilmiştir.

Dördüncü bölümde ise, HXXX programının ileriki aşamalarında uygulamaya koyulan direksiyon kolon dizayn değişiklikleri bir prototip araç üzerinde uygulandıktan sonra, yeni direksiyon ve kolon modlarının belirlenmesi için gerçekleştirilen deneysel modal analize yer verilmiştir. İyileştirilmiş direksiyon kolon bağlantı braketi ile, daha sabit ve rijit bir bağlantı sağlanması ve aynı zamanda kolon kuvvet etkisi altındayken, kolonun destekleyici yapıdan (gövde) tam olarak ve verimli bir şekilde serbest kalmasına izin veren bir bağlantı amaçlanmıştır. Biri direksiyon araç üzerinde montajlıyken, ikincisi direksiyon demonte edilerek serbest serbest sınır koşullarında olmak üzere iki modal test gerçekleştirilmiştir. Birinci test ile, yapılan dizayn değişiklikleri sonrası direksiyon kolon modundaki değişimin tespiti amaçlanmıştır. İkinci test ile direksiyon simidinin modlarının belirlenmiştir. İkinci testten elde edilen sonuçlar, sonlu eleman modellemesi korelasyonu için kullanılmıştır. Modal testlerde, kuvvet direksiyon simidi üzerindeki bir noktadan uygulanmış olup, ölçümler direksiyon simit ve kolonu üzerinde çeşitli noktalardan üç eksenli ivmeölçerler ile x, y ve z yönleri için alınmıştır. Test sonuçları bir modal test data işleme yazılım programı aracılığıyla her ölçüm noktasına ait frekans cevap fonksiyon grafikleri ve stabilizasyon grafiği yardımıyla elde edilmiştir.

Beşinci bölümde, araç kabin sonlu eleman modeli kullanılarak yapılmış olan sonlu eleman analizi sonuçlarına yer verilmiştir. Test sonuçları yardımıyla modelde modifikasyonlar yapılmış olup, direksiyon ve kolona ait model değişiklikleri

verilmiştir. Direksiyon simit modelinde iyileştirmeler yapılarak, sonlu eleman analizi sonuçları ile test sonuçları korele edilmiştir.

Altıncı bölümde ise sonuçlar ve gelecekte yapılması planlanan çalışmalar hakkında bilgi verilmiştir. Direksiyon kolunda yapılan dizayn değişiklikleriyle (braket değişikliği ile cıvata eklenmesi – 2,4 Hz), kolon 1. modunda 4,4 Hz artış sağlanmıştır. Direksiyon modeli iyileştirmesi sonrası direksiyon ve kolon 1. modlarında korelasyon sağlanmıştır.

1. INTRODUCTION

1.1 Purpose of Thesis

The steering wheel is one of the essential components of the human-machine interface in the vehicle. In automotive many customer concerns regarding noise, vibration and harshness (NVH) are related to the steering system. The steering wheel vibration is an important source of discomfort, annoyance and fatigue during driving since the driver is holding the steering wheel at all times while driving, and any vibrations from the tire nor suspension are transferred to the steering components. The acceleration magnitudes measured at the steering wheel are several times higher, and also contain more energy, than vibrations measured at the seat or the floor panel [1]. Vibration related concerns can be caused by many different components, including components in the powertrain, suspension, tire and wheels.

Since it has plenty of contributing factors, steering wheel vibration is a compelling phenomenon in the field of automotive NVH engineering. The main objectives of this thesis are to develop a good understanding of potential sources of steering wheel vibration, obtain modal frequencies and parameters of the steering wheel of a particular heavy commercial vehicle model program code named HXXX by use of finite element vibration analysis and modal impact hammer test and correlation of steering wheel model.

During the development phase of the truck which is under consideration, numerous tests and analyses had been performed to determine the main cause of the vibration. In consequence of these studies, improvement was achieved in vibration levels but it was not eliminated to a negligible level. In this paper, detailed analysis was carried out to see the characteristics of the source and response systems. In this paper, detailed analysis was carried out to see the characteristics of the source and response system and CAE model correlation study as one of the most important factor as an initial step for design improvement has been carried out.

1.2 Literature Review

There have been several detailed studies on steering wheel vibration to determine its sources, methods followed to detect the causes and to improve steering wheel vibration. Analysis and experiments had been conducted to understand what mainly causes steering wheel vibration and possible solutions that could help to minimize steering wheel vibration and several improvement methods had been implemented.

Szczotka (2011), developed a simplified planar model of a passenger car steering system and applied nonlinear optimization methods to select parameters to minimize vibrations of steering wheel. As a conclusion of the study it is revealed that the steering-suspension geometry has quite large influence on the steering kickback [2].

Kim, Grenier, Cerrato-Jay (2008), conducted a study by numerical and experimental methods on shudder vibration of a hydraulic power steering system during park maneuver. A CAE model for steering wheel vibration analysis was developed and compared with measured data. Vibration mechanism from pressure variation at power steering pump outlet to steering wheel vibration was shown through Eigen value analysis of the model. Using the developed model, an optimization was conducted and important factors were presented. It had been found out that the source of the vibration is engine rpm variation due to engine firing. The rpm variation excites the shudder mode which induces the steering wheel vibration. Peak amplitude of steering wheel angular acceleration was determined as the most important factor in perception of shudder [3].

According to Mangun (2006), excessive torsional vibrations in steering system mainly caused by nonuniform tire/wheel assembly producing periodic force variations. A parameter sensitivity study was performed and it was shown that through proper tuning of the inertial and frictional properties of the steering system and suspension parameters, the vibration transmission could be substantially decreased [4].

Sugiyama and Krishige (2006), presented a new control strategy for electric power steering which they developed to reduce steering vibration associated with disturbance from road wheels [5]. Zhang, Ning and Yu (2007), investigated steering wheel vibration caused by brake judder. Tests conducted under controlled braking conditions, modeling and simulation were carried out to reproduce and explain the

vehicle road test and brake dynamometer test. A multi-body-dynamic vehicle model with a full description of tire road friction, suspension and steering system, rubber bushings and vehicle inertia was also established in ADAMS to predict and validate of the influences of various factors from disc brake system, suspension system, steering system and tire which can be used for chassis design to control steering wheel vibration due to brake judder [6].

Matsunaga and Nishimura (2001), constructed a mathematical model for a hydraulic power steering system and performed numerical analysis for self-excited vibration caused by rapid steering in the power steering system. From the examination, the guide of the prevention against the vibration was derived, such as positioning the rather long hose at near the power steering gear in the supply line [7].

Wang et al. (2013) used vibration tests and modal analysis method to recognize cause of steering wheel's idle shaking. It was found that the steering wheel's operating modal was close to engine's second order excitation frequency, which caused steering wheel's idle shaking. Five improvements were presented including structural optimization, lightweight design of steering wheel, installation of dynamic vibration absorber, matching of power train mount and reduction of engine idle speed, the effectiveness and rationality of the improvements was verified through experiments [8]. Demers (2001), developed a methodology for the diagnosis of vibrations of the steering wheel and went through what the sources of steering wheel vibrations might be, and how various steering system parameters might affect the vibrations. Analysis resulted that, there was a direct relation between the tie rod (road wheel) and vibrations below 20 Hz and vibration in the 80-90 and 120-150 Hz regions, direct relation between the steering rack and 18-25 and 29 Hz vibrations and in the 80-90 Hz region and direct relation between the instrument panel (cross-car beam) and 10-40 Hz vibrations and in the 100-200 Hz range [9].

Kim et al. discussed the vibration characteristics of steering wheel in front drive small-sized passenger cars. Measurements of vertical and lateral accelerations at the steering wheel were taken from a small sized passenger car on typical road. The effect of engine vibration, road excitation and structural system characteristics are identified by experimental and analytical methods. A significant reduction in the vertical vibration is demonstrated in the data and has been achieved using several improvement in the structure and system [10].

Also numerous studies had been conducted in order to determine natural frequency of various steering systems and to investigate the nature of steering wheel vibration using FEA or experimental methods. Optimization studies had been carried out to reduce steering wheel vibrations. Botti, Venizelos and Benkaza, developed an approach in how to optimize upfront at the early design stage the instabilities of a power steering system for passenger cars by using specialized computer simulation. The rotary spool valve excitation through the the pump excitation was the main cause for low frequency disturbances up to 100 Hz. It was suggested that it is necessary to reduce the vibrations within the rotary spool valve in order to avoid transmissibility of pressure pulsations into the steering rack and the consequence would be a drastic reduction of the vibrations through the suspension and the body structure [11].

Sul et al. (2011) investigated vibration problem of a middle sized passenger car under idle condition by testing and analysis. The root reason for the severe vibration of the steering wheel under the idle conditions was found. Study results shows that, steering wheel first order natural frequency was too close to the engine's second order frequency and resulted with steering wheel vibration. Modal separation was achieved by improving the system's structure to avoid the severe jitter of the steering wheel caused by resonance, and the problem was solved effectively [12].

Slave et al. (2008) used CAE models validated by experimental measurements to identify modes of vibration of a cab of a truck and vehicle which have significant influence on steering column response. The vibration observed in the steering column was not a consequence of a mode of vibration of the column itself, but a vibration of the whole vehicle front end was inducing the vibration. Significant vibration amplitude reduction on CAE analysis was observed as a result of addition of a lateral link (Panhard) between cab front end and chassis first cross member, in order to eliminate cab yaw movement from front axle roll mode of vibration [13].

Chen et al. (2012) created a model of the steering system based on FEM to understand the vibration characteristics of the system. First twenty step modes of the system were calculated and analyzed by modal analysis. Study resulted that the frequency of the first step mode is 31.578 Hz which is higher than the exciting frequency of the engine; also, the road roughness excitation frequency has a minor influence on steering wheel vibration [14]. Guo et al. (2012) established a three-dimensional FEM of a steering wheel and conducted finite element static and dynamic analyses in order to validate

dynamic characteristics and strength of the steering system [15]. Xiang and Yinxiao (2012), built a three-dimensional model of automobile electric power steering system. The structure design and dynamic characteristic optimization of the model were researched, and on the basis of natural frequencies analysis, several design improvement schemes were brought forward to avoid the overlap of system natural frequency and the engine excitation frequencies in idling speed [16].

Bianchini (2005), described an approach of implementing a cost effective active vibration control system applied to a steering column. Bianchini designed the active control system to eliminate the engine idle vibrations being transmitted to the steering wheel. A finite element model of the structure was developed and used to size the actuators and locate the sensors. A 25 dB reduction at the target mode was achieved numerically [17].

Landreau and Gillet, analyzed steering wheel vibration through test and numerical modal analysis in their study. A dynamic mode was identified as responsible for the sensitivity of vehicle. Study deals with steering wheel vibrations which appear in straight driving case speeds between 90 and 150 kph. It was convinced that the phenomenon of angular steering wheel vibrations is mainly due to a resonance frequency of a front axle mode and control of the phenomenon can be achieved through the mastery of excitation sources as wheel unbalance and radial non-uniformity and optimized axle design [18].

Zhang and Dong (2012), built a steering mechanism simulation model and studied dynamics simulation analysis using the multi-body system dynamic method. A flexible tie-rod model and a rigid-flexible coupling steering mechanism model were built and natural modes attained by ANSYS. The dynamic characteristics of the multi-body rigid model and the rigid-flexible coupling model were compared. The accurate simulation results of the rigid-flexible coupling model were verified by simulation test [19].

Othman (2011), suggested that major cause of the steering wheel vibration is engine vibration while the steering wheel vibration level is different for every steering wheel model depending on its shape, design, weight, material and size. Three different experiments conducted to investigate the nature of steering wheel vibration consisting experimental study of modal analysis for a steering wheel in free-free boundary condition, experimental study of modal analysis for a steering wheel in constraint

condition and experimental study on highest vibration for a steering wheel in dynamic condition [20].

Shim and Shin (1999), presented design process for high stiffness steering system using light weight magnesium alloy and final results improved about 10 dB level [21].

Kim, Choi and Kim (2007), described the optimal design process of the steering column system and the supporting system. Case studies on resonance isolation were summarized, in which separated vibration modes among systems by applying Vibration Mode Map at the initial stage of design process. Study, also provided design guideline for optimal dynamic damper system using computer aided engineering (CAE) analysis. The damper finite element (FE) model was added to vehicle model to analyze the relation between the frequency and the sensitivity of steering column system which enables target performance achievement in early design stage and reduction of damper tuning activity after proto car test stage [22].

Abreu and Moura (2012), used techniques as mechanical vibration analysis, operational modal analysis and operational deflection shape to identify the root cause of increased levels of vibration felt at idle speed in a popular vehicle prototype. Study demonstrates the methodology used to identify the cause of the different behaviors between cars and improvements made in the body according to the results of the numerical experimental confrontation [23].

Britto et al. (2013) discusses about methodology of steering assembly development for NVH performance of commercial vehicle. It dealt with steering wheel targets setting and cascading it to system, subsystem and component level targets and achieving these targets by collaborative Test-CAE approach. Target verification and achievement have been done by using bottom up approach starting from component, sub-system, full vehicle level modal targets for tilt and telescopic steering assembly. Steering wheel vibration levels were evaluated for power train idle and wide open throttle (WOT) condition and the design is further refined to meet the targets. Baseline steering wheel and steering assembly was correlated with the experimental results based on modal frequencies and mode shapes [24].

Fujiwara and Nakayasu (1971), made an analysis of vibration phenomena in the steering system of a vehicle, when the front wheels have some amount of unbalance. The influences acting on rotational vibration at the steering wheel end by varying each

factor in the vibration system were determined by actual running tests. More detailed experimental investigations were made using a rolling drum and by bench test. From the data accumulated through these experiments, some important factors in the vibration phenomena were selected, and a mathematical model incorporating all these parameters was simulated on a digital computer [25].

Sugita and Asai, described an experimental method for the reduction of the steering wheel vibration, occurring at high speed cruising and/or at engine idling. The reduction of the vibration can be achieved by increasing the resonant frequency of the steering system, which was constructed of a steering wheel, steering column, its support member and so on. Mechanical impedance methods were applied to predict the resonant frequency by means of converting the diametrical moment of inertia of the steering wheel into an equivalent mass. This method provides an insight into how design should be changed to obtain further reduction of the steering wheel vibration [26].

Kim and Choi, studied several steering wheel vibration problems and detailed analysis was carried out to see the characteristics of the source and response systems. A dual mode steering wheel dynamic damper was developed to control the shake and shimmy problems. By using experimental and analytical methods its design parameters were tuned to damp out both vibration problems. Experimental results after applying this damper showed a comprehensively good attenuations of both vibration levels of steering wheel which also showed a possibility of control two different vibration problems using only one dynamic damper without increasing weight and cost [27].

Min et al. (2012) investigated the shimmy mechanism caused by self-excitation components of a vehicle identified at 120 km/h. The operating deflection shape (ODS) analysis used for the chassis from 90 to 140 km/h. The front right lower arm is identified as the shimmy cause by analysis of movement characteristic change of the chassis components [28].

Shi et al. investigated the cause of steering wheel's idle shaking through vibration test and modal analysis method. It was found that steering system's operational modal was close to the 2nd order excitation frequency of the engine, and steering wheel resonated. To relief this problem, five improvements were presented, including structure reinforcement, lightweight design of steering wheel, installing of dynamic vibration

absorber, matching of power train mounts and increase of engine idle speed. The effectiveness of each improvement was proved through experiments [29].

Xie et al. proposed the test and simulation integrated transfer path analysis and optimization method to decrease the steering wheel vibration in idle. First the contributors to the steering wheel vibration were studied, including the vibrational excitation sources, the transmission channels, and the steering wheel itself. Then a series of improvements were carried out, including lowering the engine idle speed with AC on, tuning the engine mounts to decrease the engine vibration, improving the body structure and the support brackets of the steering column, etc. Results showed that the steering wheel vibration in idle drops over %70 [30].

Giacomin J. et al. investigated the human perception of rotational hand-arm vibration by means of a test rig consisting of a rigid frame, an electrodynamic shaker unit, a rigid steering wheel, a shaft assembly, bearings and an automobile seat. Fifteen subjects were tested while seated in a driving posture. A frequency weighting was developed for the purpose of evaluating steering wheel rotational vibration [31].

According to Ereke (1986), in the process of development of less sensitive axle and steering wheel system, subjective assessment of the driver's perception of the vibration should also be a concern as well, besides the endeavour of reduction in the acceleration values. Therefore, a series of surveys had been conducted with many drivers and as a result of these surveys some criterion revealed regarding subjective evaluations [32].

Jeon (2010), performed experimental activities in order to answer questions about the quantification of the human subjective response to automotive steering wheel vibration, and to use the findings to define a test method for automotive steering wheel hand-arm vibration [33].

You et al. (2011) used two passenger cars to evaluate the subjective rating of steering wheel vibration. Acceleration data were measured from a steering wheel during vehicle operation at several speeds over various types of roads. The component values of the measured acceleration were filtered by the weighting function defined in ISO 5349-1, and then they were summed to calculate the overall values. Correlations were determined between the weighted accelerations and the subjective ratings of four expert drivers and ten general drivers using Stevens' power law [34].

1.3 Hypothesis

Today's engineering design needs to manage the conflicting goals as increasing performance while reducing developing time and costs. To meet these challenges, tests have to be defined and prepared as much as possible before the prototype is available and large amounts of test data have to be acquired and evaluated while avoiding errors. Preparation of component of vehicle models and analysis of their performance in terms of structural integrity is a key to fast simulation of new designs. Dynamic behaviours of components, assemblies and complete vehicle can be accurately calculated under a wide range of conditions, for example idle and on road. In the highly competitive automotive industry, efficient analyses are vital to improving design and increasing the cost-effectiveness of the development process [35, 36, 37].

This paper discusses the combined usage of CAE and test to speed up the development process. This paper presents the correlation of the results of steering wheel vibration testing performed on a particular truck and FE modal analyses.

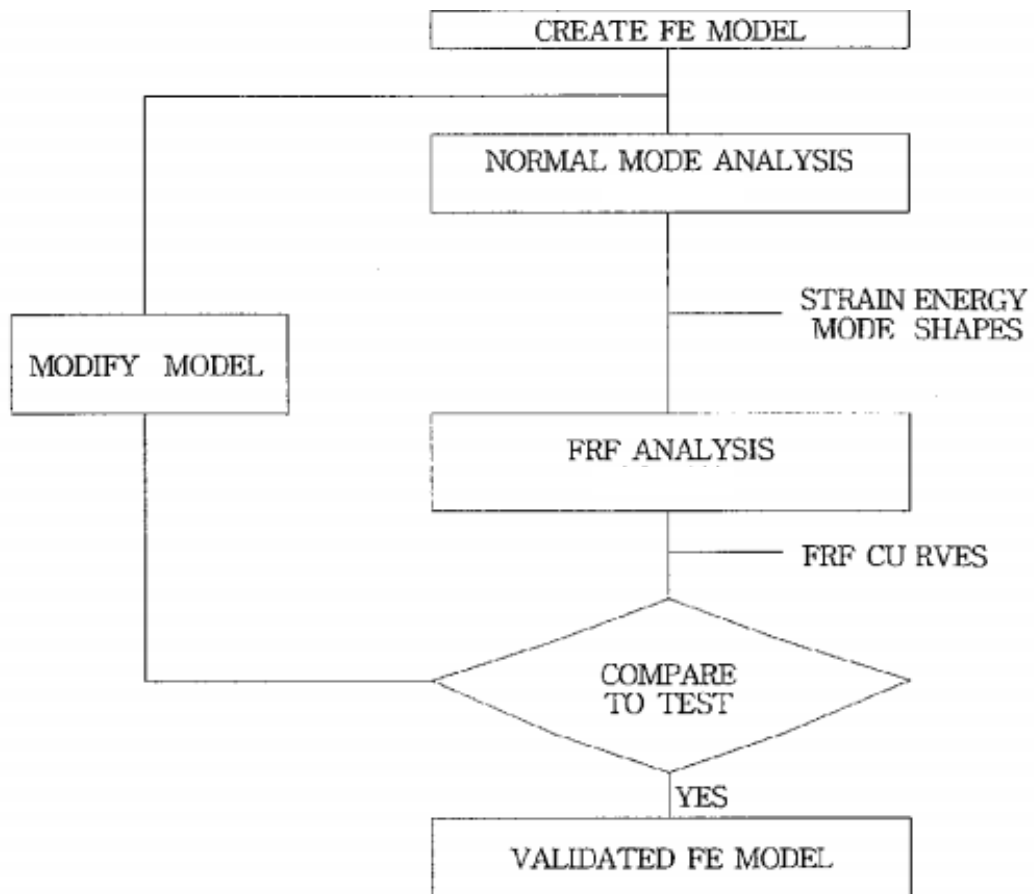


Figure 1.1 : FE model correlation process.

2. SOURCES OF STEERING WHEEL VIBRATION

2.1 Steering System Decomposition in Heavy Commercial Vehicles

For a better understanding of potential root causes of steering wheel vibration in a heavy commercial vehicle, systems and components, which may have a transfer path to the source of the vibration to the steering wheel, will briefly introduced in this section.

A steering system is designed to enable the driver to control the traveled path of a vehicle. The steering system must give the operator some form of which would allow him/her to feel about the load condition that the tires of the vehicle experiences. This feedback is very important for the driver to easily control the direction [38].

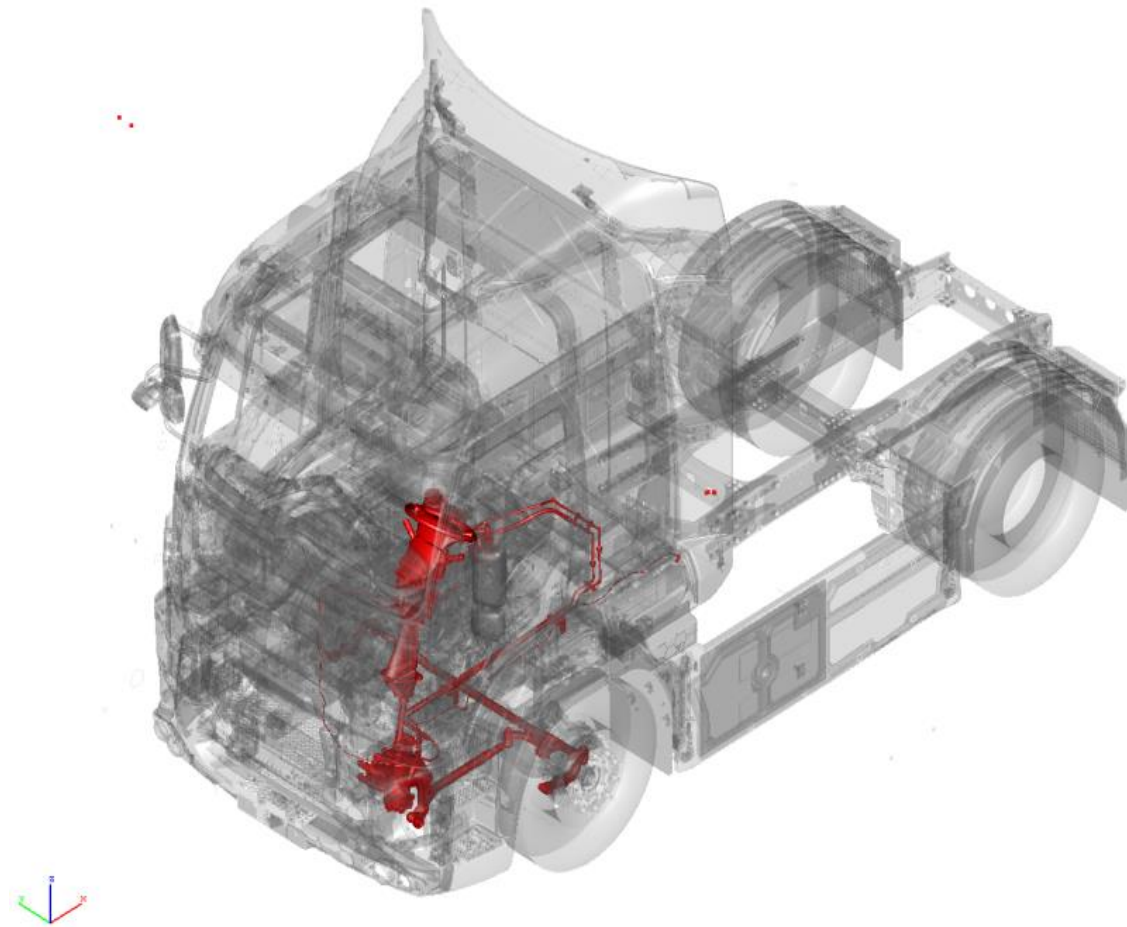


Figure 2.1 : HXXX CAE model.

Main components of the steering system of a truck are steering wheel, steering column, steering gear, and steering linkages including Pitman arm, drag link that move the steering tires.

The steering wheel is the instrument used by the driver to control the directional tracking of the vehicle. Therefore, steering wheel is the primary input to the steering system. The steering wheel used on a truck supported by spokes extend from the wheel hub, which turns on a bushing or bearing at the top of the steering column.

The steering column connects the steering wheel to the steering gear. The main function of steering column is to transfer the rotational moment from the steering wheel to the steering gears. The steering column is usually sectional (retractable) and designed to collapse in the event of a collision. The typical vehicle requires about three complete revolutions of the steering wheel to rotate front wheels from full left to full right. The steering wheel is bolted to splined steering shaft in the steering column. The steering column consists of the jacket tube called as steering housing fixed to the body and steering shaft (also called steering tube).

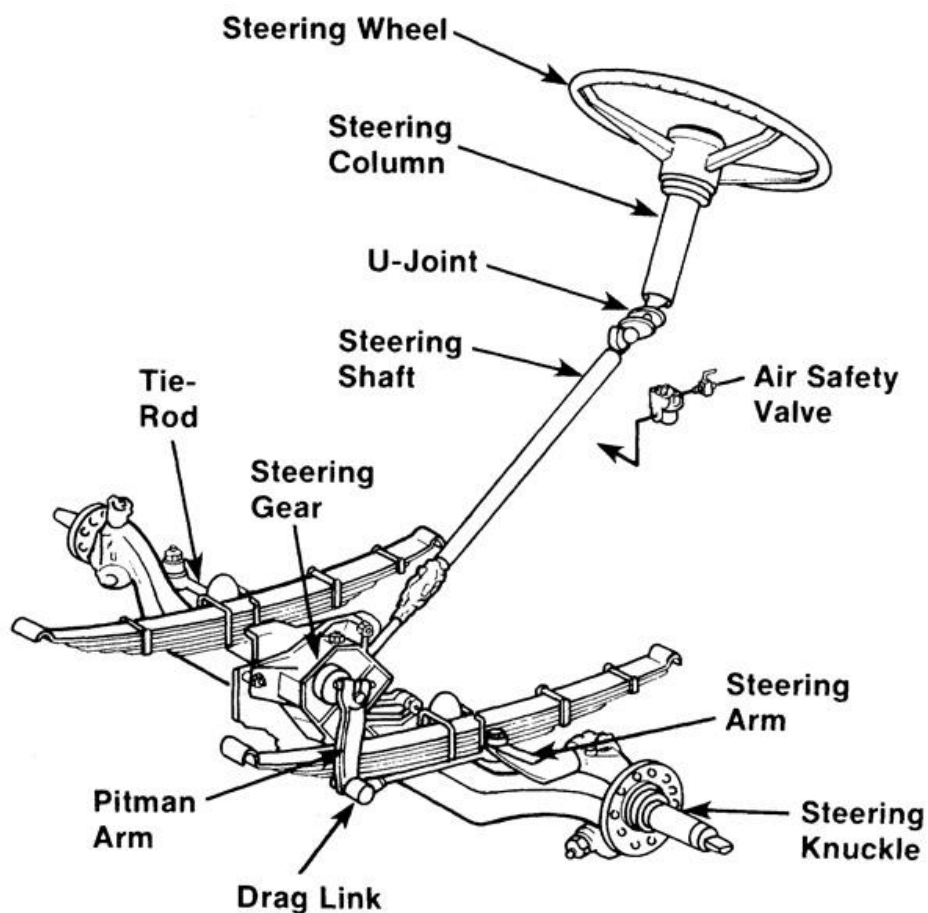


Figure 2.2 : Steering system components of a truck [39].

The major components of the steering column assembly are tube, bearing assemblies, a steering column shaft and wiring and the contact assemblies for the electric horn. The steering column assembly is mounted to the dash steering column bracket by support brackets located under the cover housing. Coupled to the steering column upper shaft by a pair of yokes and the U-joint assembly is the lower shaft assembly. The U-joint permits some angular deviation between the upper and lower column shafts. The lower column assembly connects to the steering gear.

A Pitman arm is a steel lever, splined to the sector shaft of the steering gear. The end of the Pitman arm moves through an arc with the sector shaft center forming its center. The Pitman arm functions to change the rotary motion of the steering gear sector shaft into linear motion.

A drag link is a forged rod that connects the Pitman arm to the steering control arm. The drag link can be a one or two piece component. The length of two piece design is adjustable, which makes it easy to center the steering gear with the wheels straight ahead. The drag link is connected at each end by ball joints. These ball joints help isolate the steering gear and Pitman arm from axle motion.

The steering control arm connects the drag link to the steering knuckle on the driver side of the vehicle. When the drag link is moved in a linear direction, the steering control arm moves the steering knuckle, which changes the angle of the steering knuckle spindle.

Steering knuckles mount to the rigid front axle beam by means of steel pins known as kingpins. They provide the ability for the pivoting action required to steer the vehicle. The steering knuckle incorporates the spindle onto which wheel bearings and wheel hubs are mounted, plus a flange to which the brake spider is bolted. A steering control arm is attached to the upper portion of the left side steering knuckle and tie-rod arms are attached to both left and right steering knuckles.

Tie-rod arm is the means used to transfer and synchronize steering action on both steer wheels on a steering axle.

The steering arm or lever controls the movement of the driver side steering knuckle because it connects directly to it. The steering knuckles are required to be connected to each other so they act in unison to steer the vehicle. Transferring this steering motion

to the passenger side steering knuckle is achieved by using a tie-rod or cross tube assembly.

Axle beam steering system consists of a steering wheel, which imparts motion to the steering box. This conveys the steering effort through the Pitman arm and drag link directly to one of the two stub axles pivoting at the ends of the axle beam. A track rod joins both the stub axles together. Figure 2.2 shows the axle beam steering layout in three dimensional view showing each component and its relative position within the system. The steering box provides a gear reduction so that, with only a small effort, a much larger force can be applied to the steering linkage. At the same time, the degree of stub axle movement will be reduced for a given angular movement of the steering wheel. This is desirable as it prevents the steering being oversensitive to the drivers touch on the wheel. With the rigid beam suspension, a stub axle is pivoted at each end of the axle beam so that relative movement can take place only in the horizontal plane. Therefore, the effective track rod length is not influenced by any vertical suspension deflection [39].

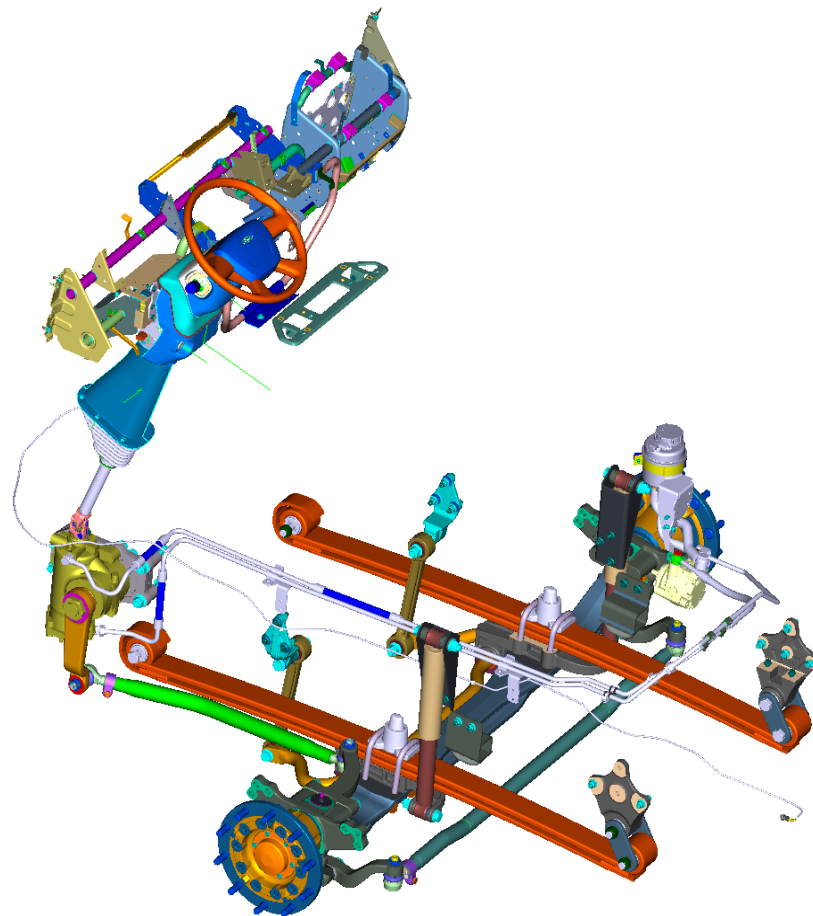


Figure 2.3 : HXXX axle beam steering and suspension system.

2.2 Sources of Steering Wheel Vibration of Heavy Commercial Vehicles

Steering wheel vibration is affected by various internal and external vibrational sources. The internal sources are the rotational irregularity of the engine which is caused by both the stochastic combustion forces and the dynamic unbalance of components such as the translating pistons. The external sources include the road surface irregularities and the aerodynamic forces. For both the internal and external sources the vibration which actually reaches the driver is moderated by the dynamic response of the automobile chassis components.

Figure 2.4 presents the three principal vibrational axes of the steering wheel defined by standard SAE J670e (1976). The vibration at the steering wheel is normally measured along three axes. The X axis is taken along the fore-and-aft direction of the automobile with the positive direction taken as forwards, i.e. from the driver towards the front bumper. The Y axis is taken along the lateral direction of the automobile with the positive direction towards the left of the vehicle. The Z axis is taken along the vertical direction of the automobile with the positive direction towards the roof of the vehicle.

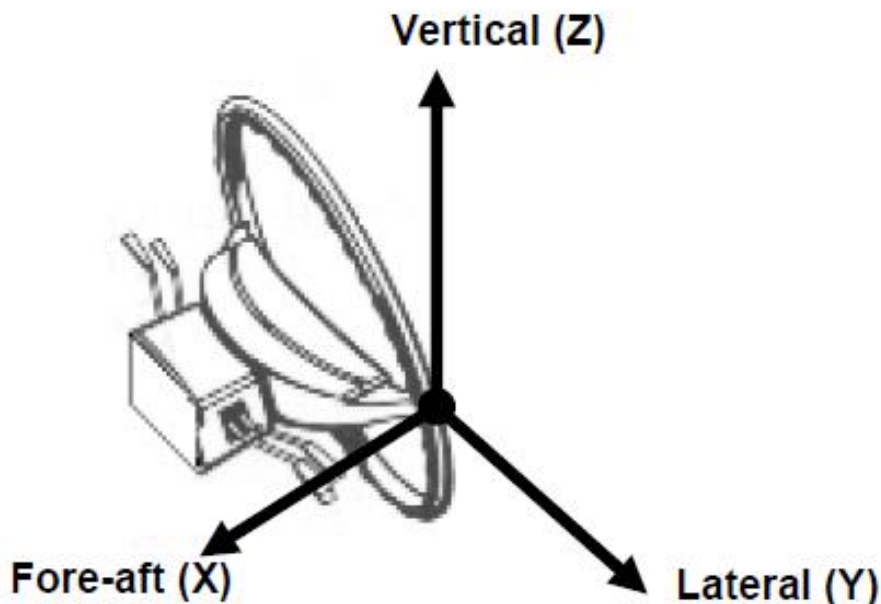


Figure 2.4 : Three axes of vibration measured on a steering a wheel [34].

Steering wheel vibration can reach frequencies of up to 300 Hz during driving and vibrational modes of the wheel and column can produce large resonant peaks in the steering wheel power spectrum at frequencies from 20 to 50 Hz. Although steering

wheel vibrations do not normally exceed levels which present a health risk in automobiles and trucks, such vibrations nevertheless can cause discomfort, annoyance and physical or mental fatigue [33].

The vibration phenomena generated in a vehicle steering system can be classified as forced vibrations such as flutter, kickback etc. and self excited vibrations such as shimmy. Flutter is a stationary vibration generated by a periodic external force due to an unbalanced front wheel, etc. while kickback is transient vibration generated by an external force due to unevenness of the road, etc. Shimmy, on the other hand, is vibration generated by dynamic characteristics of the tire, etc. [25].

The major mechanical oscillations are road induced (uneven road), tire induced (unbalance tire/wheel) and powertrain induced (engine idle shake, driveline unbalanced). These oscillations are transmitted through the chassis to the passenger compartment, generating a wide range of coupled oscillation modes, which in turn are amplified (resonance) or reduced (damped), depending on the natural frequencies of each of the vehicle components [40].

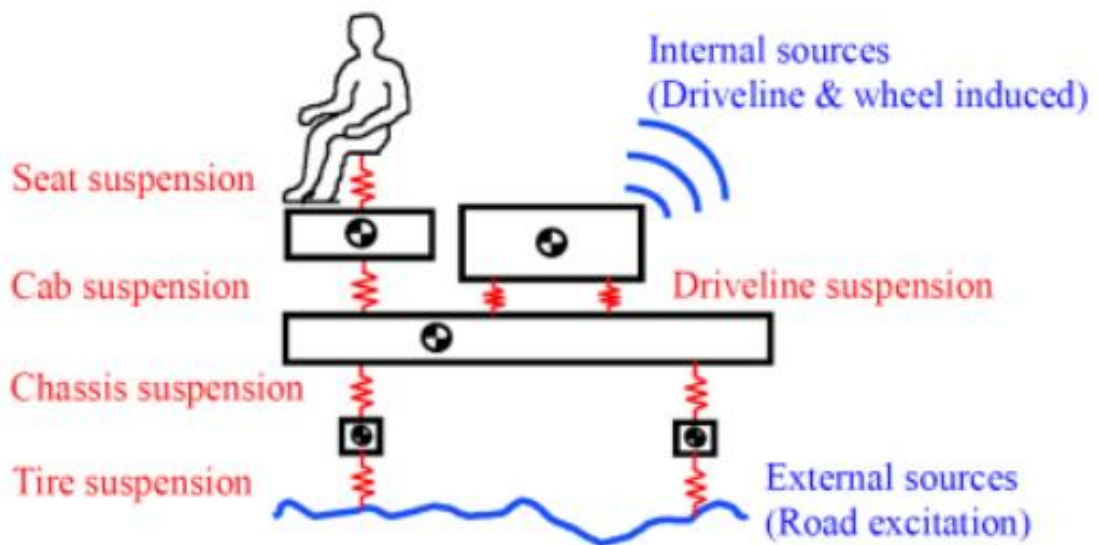


Figure 2.5 : Sketch of the main suspension systems and vibration sources of a heavy truck [41].

Oscillations are experienced as comfort disrupting in the frequency range 0-25 Hz. Oscillations with a frequency higher than 25 Hz are experienced as noise.

Kim et al. listed vibrational source of steering wheel vibrations as engine vibration by unbalance and torque fluctuation, wheel and tire vibration due to the unbalance of drive train and nonuniformity of tire and road surface irregularity [10].

2.1.1 Brake judder (Shudder)

Brake judder is a kind of low-frequency brake vibration and noise phenomenon. Normally, brake judder has a peak at 60 to 80 kph and has a frequency of 5 to 30 Hz. It can cause steering wheel wobbling, instrument panel vibration, driver seat shaking and brake pedal pulsation, and sometimes the entire body to vibrate vertically and back-and-forth during braking, sometimes with a booming noise. All these will greatly affect driver driving comfort and driving safety. Brake judder may lead to huge amount of service cost and damage manufacturer's commercial competition. The prevention and control of brake judder has been a key development target firmly integrated in the vehicle development process [6].

Judder is transmitted through the brake hydraulic lines to the suspension system, steering system and the brake pedal. Brake pedal pulsation is generated when applying brake with a non-uniform brake disc thickness.

Certain operating conditions can affect the cause of these vibrations. These include, extended periods where the vehicle is not in operation, brake disc surface irregularities due to foreign agents (oil or grease, antifreeze etc.) and deformation of brake drum due to poor installation.

If the disc rotor has excessive thickness variation, friction force on the braking surface varies during brake application. The change in the braking force generates a vibration at a certain frequency. This vibration is transmitted to the suspension, steering and brake pedal the vibration can also transmit to the body, causing it to resonate.

Generally it is known that brake judder is excited by disc thickness variation (DTV) and disc sideface runout (SRO), or thermoelastic instability (TEI) of brake with ideal geometric disc. They are termed cold judder and thermal judder respectively. Hot judder is usually produced as a result of longer, more moderate braking from high speed where the vehicle does not come to a complete stop. It commonly occurs when the driver decelerates from speeds of around 120 km/h to about 60 km/h, which results in severe vibrations being transmitted to the driver. These vibrations are the result of uneven thermal distributions, or hot spots. Hot spots are classified as concentrated

thermal regions that alternate between both sides of a disc that distort it in such a way that produces a sinusoidal waviness around its edges. Once the brake pads (friction material/brake lining) comes in contact with the sinusoidal surface during braking, severe vibrations are induced, and can produce hazardous conditions for the person driving the vehicle.

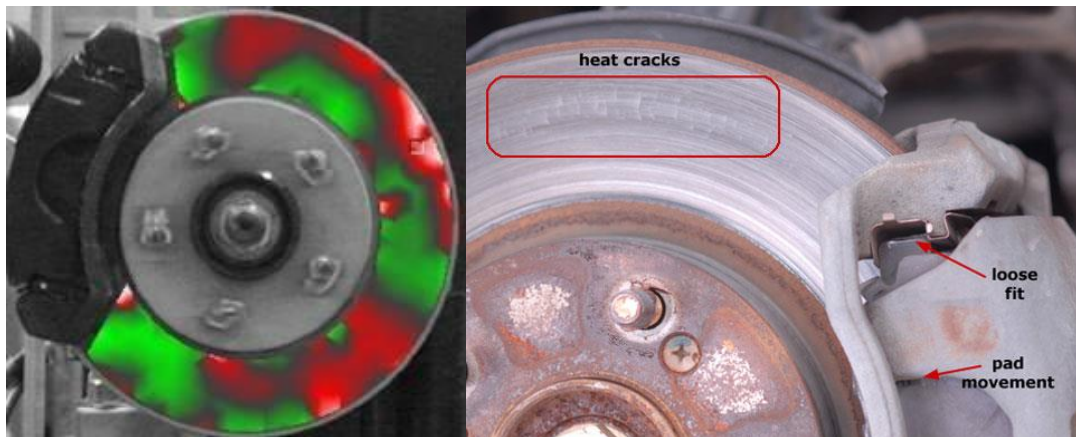


Figure 2.6 : Uneven thermal distributions on disc brake.

Cold judder, on the other hand, is the result of uneven disc wear patterns or disc thickness variation (DTV / Runout). These variations in the disc surface are usually the result of extensive vehicle road usage. DTV is usually attributed to the following causes: waviness and roughness of disc surface, misalignment of axis (runout), elastic deflection, wear and friction material transfers.

Also suspension and steering system play important role in the brake judder induced various vehicle NVH as vibration transmission path. Thickness variation can be caused by a rotor that has lateral runout. Lateral runout can be caused by improper wheel tightening procedures and torque values as well as hub runout. As the rotor wobbles, (lateral runout) contact is made with the brake pads. As sections of the rotor make contact with the pads, small amounts of metal wear from the rotor surface. This continues until enough metal is worn in sections to cause thickness variation [6].

Vibrations are noticeable at the steering wheel, seats and floor. The level and intensity of the vibration changes with the suspension type and the bushings used.

The rigidity of the bushings and insulators in the vibration transmission path has a large influence on harshness. The use of low-rigidity bushings and insulators to

provide greater fore-aft suspension compliance softens the impact force effectively, but results in less responsive steering.

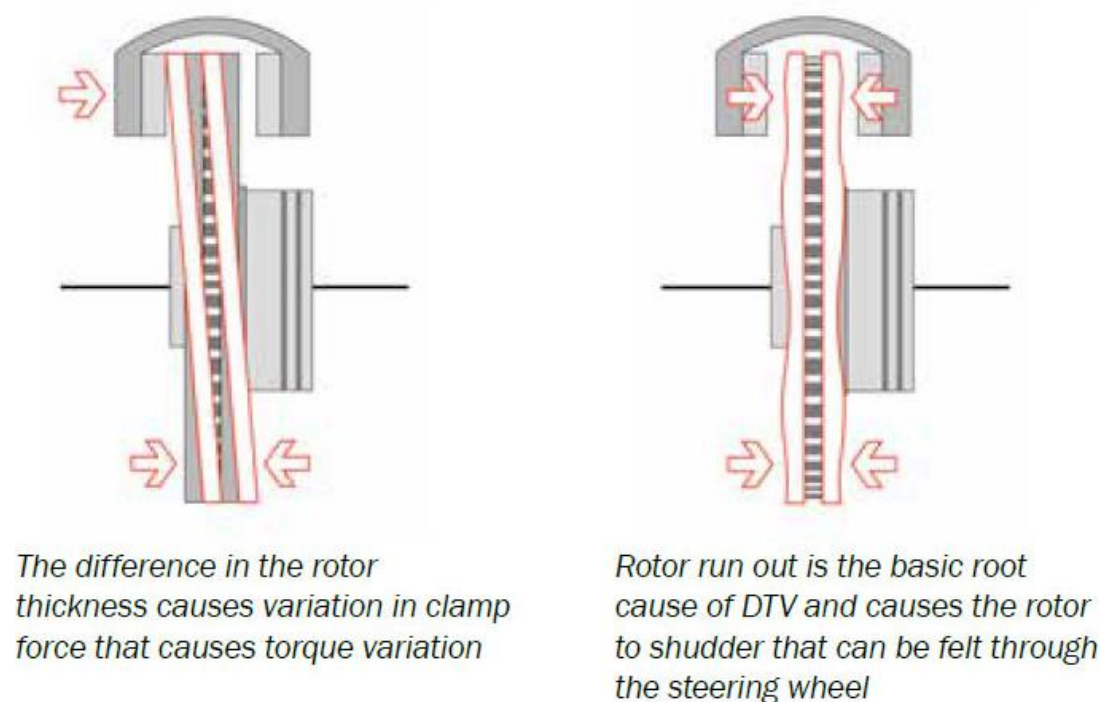


Figure 2.7 : Disc brake thickness variation.

2.1.2 Shimmy and nibble

Nibble is a rotational vibration at the steering wheel that occurs at highway speeds and is caused by vehicle sensitivity to tire and wheel force variation. Nibble is perceived by the driver as a vibration at the steering wheel when driving at highway speeds [42].

The periodic force variations produced by a nonuniform tire/wheel assembly are known root causes of excessive torsional steering wheel vibrations known as steering nibble [4].

Vibration that causes the steering wheel to oscillate is known as shimmy. The body of the vehicle also may vibrate laterally. Shimmy generally has a frequency of 5 to 15 Hz (mostly 8 – 12 Hz). Shimmy can be described as a sustained oscillation of both front wheels about the kingpin axis which can result in a severe lateral shake of the vehicle and/or steering wheel oscillation. It is generally associated with solid axle front suspensions. Shimmy is more prevalent with steering systems that do not have a damping element in the load path between the right and left steering arms (e.g. ball nut

steering systems or manual rack and pinion). Shimmy typically occurs at moderate vehicle speeds. Shimmy can be both experienced as high-speed or low-speed shimmy.

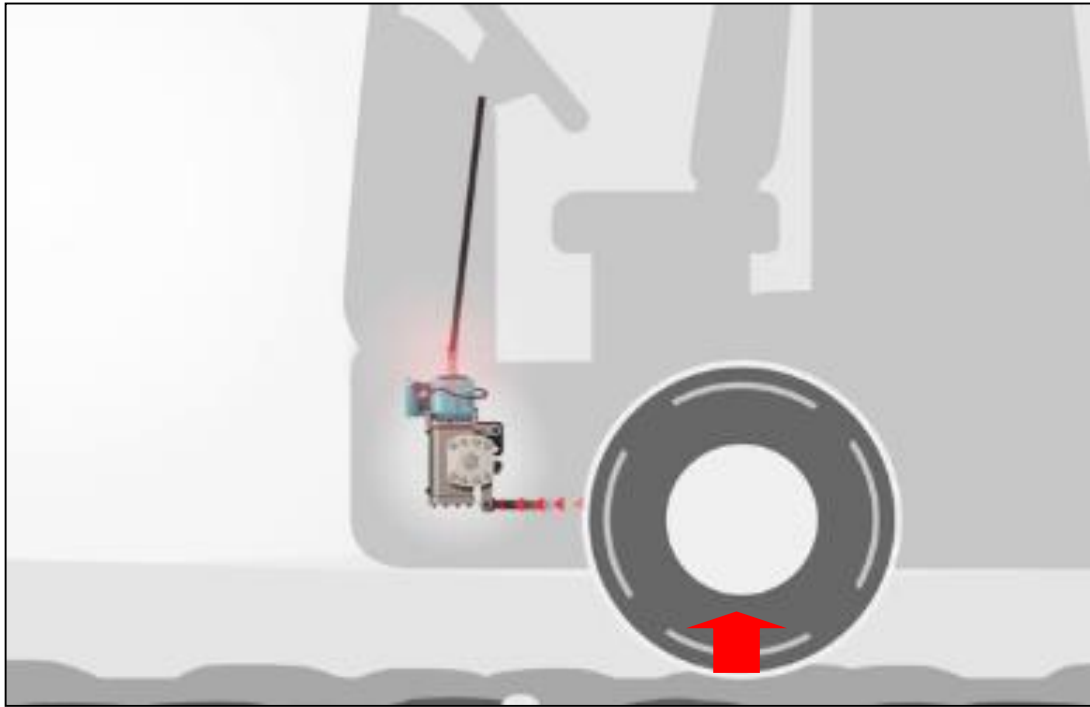


Figure 2.8 : Steering wheel vibration due to road roughness.

High speed shimmy occurs when driving on smooth roads at high speeds. High speed shimmy typically has a limited speed range in which symptoms are noticeable. Low speed shimmy occurs when the steering wheel begins to vibrate as the vehicle is driven across a bump at low speeds.

The major vibration sources of high speed and lowspeed shimmy are roughness of road, tire imbalance, non-uniform tires and bent or out-of-round wheels.

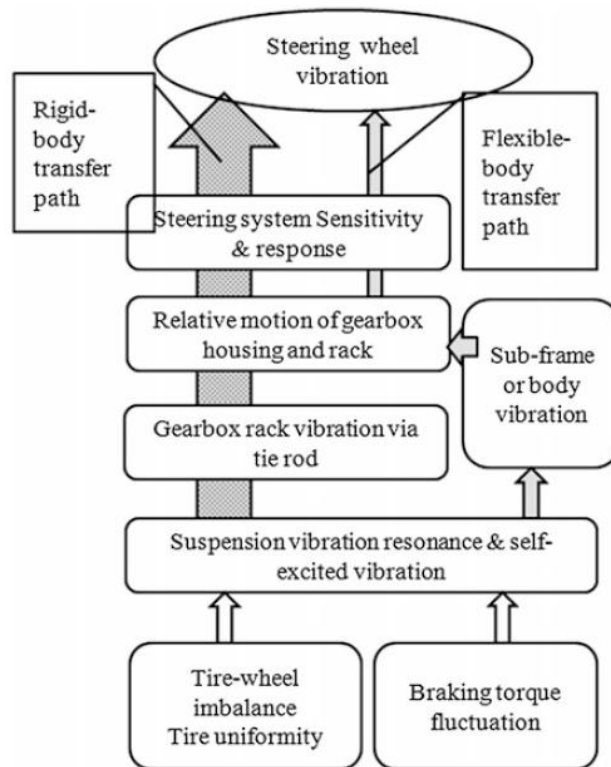


Figure 2.9 : Transfer path of steering shimmy and brake judder [28].

For example, a tire with excessive runout, out of balance, or out of round wheels may cause high or low-speed shimmy. This is because the tire fault generates a vibration at a particular frequency. When the vibration of the tire reaches the natural frequency of the vehicle's front unsprung components (such as the front axle, tires, and wheels), they start to vibrate. When the frequency of the front unsprung components matches the natural frequency of the steering system, resonance occurs. This resonance causes the steering wheel to vibrate heavily in the turning direction.



Figure 2.10 : Steering wheel shimmy and nibble.

2.1.3 Shake and idle shake

Vibrations at the steering wheel or seat, or an annoying vibration at the floor, are indicators of shake. Shake generally has a frequency of 10 to 30 Hz. Shake can be vertical (up and down) or lateral (side to side).

Vertical shake is severe vertical vibration of the body, seats and steering wheel. A trembling engine hood or rearview mirror also can be a vertical shake symptom.

Lateral shake is side to side vibration of the body, seats and steering wheel. A trembling vibration in the driver's waist or hips may be a symptom of a lateral shake.

The major vibration sources of vertical and lateral shake are roughness of road, tire imbalance, non-uniformities, bent or out of round wheels, driveline and engine.



Figure 2.11 : Steering wheel shake.

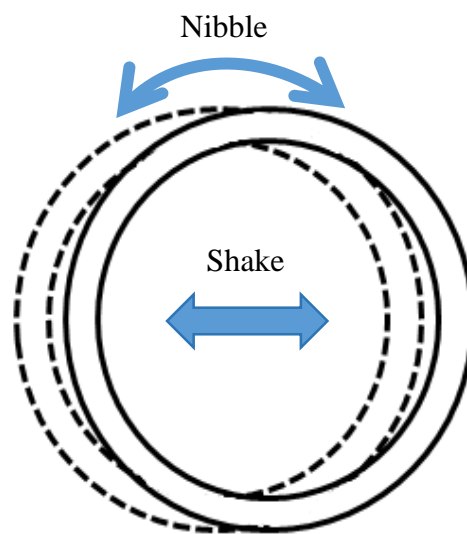


Figure 2.12 : Steering shimmy and shake [28].

4. BACKGROUND OF ROOT CAUSE INVESTIGATION OF HXXX STEERING WHEEL VIBRATION

In the process of HXXX development, during subjective evaluation phase drives, excessive vibration of the steering wheel at idle condition was identified. There are many factors that may cause the vibration in idle including the vibrational excitation sources, such as the engine and engine mounts; the transmission channels, such as the body structure, suspension and the steering wheel itself. Thus identifying the source of the vibration becomes a very complex problem. Therefore, a procedure had been applied to identify this vibration phenomenon and to search alternatives to decrease or eliminate it.

To identify the problem, a series of tests had been performed. Two of the launch vehicles were used to perform cross measurements, which were selected as worst (Vehicle A) and best (Vehicle B) cases (Table 3.1 and Table 3.2), to obtain effective parameters on the issue which can lead to root cause of the problem. Measurements were conducted on vehicles A and B during hot idle condition. In order to obtain all vibration data from steering wheel, mount active and passive sides, four iterations were performed.

Three 3-axis accelerometers, a one-axis accelerometer and a RPM transducer were used to take measurements. Three-axis accelerometers were placed at rear engine mount active side, rear engine mount passive side and at steering wheel, respectively. The one-axis accelerometer was used for reference to measure z displacement of the engine block.

Steering wheel vibration levels at idle are given in Table 3.1. According to the measurements, vehicle A has much higher steering wheel vibration level than vehicle B.

Table 4.1 : Comparison of the initial steering wheel vibration levels of vehicles A and B at idle.

	Steering Wheel Vibration Velocity (mm/s)	
	Vehicle A with Base Mounts	Vehicle B with Base Mounts
X	14,2	3,9
Y	4,8	1,2
Z	8,2	2,8
RSS	17,1	5,0

As a first step to the root cause analysis, engine vibration level had been investigated as the source of the vibration. Engine vibration levels were measured on the active side of the mount brackets to find out whether source vibration levels are different among the measured vehicles.

Table 4.2 : Engine active side bracket vibration RSS measurements.

	Vehicle A	Vehicle B
Front Left Engine Active Side Bracket Vibration (m/s²)	5,1	3,1
Rear Left Engine Active Side Bracket Vibration (m/s²)	4,5	3,1
Front Right Engine Active Side Bracket Vibration (m/s²)	4,8	3,1
Rear Right Engine Active Side Bracket Vibration (m/s²)	4,5	2,8

According to base measurements when the engine mount active side combustion related vibration levels which represents the source vibration compared, vehicle A has higher vibration levels than vehicle B. As a result of higher source vibrations, steering wheel vibration is higher on A as expected.



Figure 4.1 : Accelerometer placement on engine active side bracket.

As a transfer path effect, engine mount rubber stiffness variance was investigated by switching A and B mounts. After mount replacement it was confirmed both subjectively and objectively that vehicle A got better and vehicle B got worse in terms of steering wheel vibration.

For further investigation, former phase level mounts assembled to vehicle A and measurements performed again as former phase level mounts have lower dynamic stiffness values. Although former phase engine mounts provide better vibration isolation performance, to improve durability issue of the engine in order to constrain excessive engine movement, rear engine mounts were optimized and left and right rear engine passive side mounts had been changed. The only difference between former level rear passive side engine mounts and latest level rear passive side engine mounts is rubber composition properties. Both engine mounts have same active side and passive side brackets, however latest level rear passive side engine mounts rubber composition is stiffer than former level engine mount rubber composition. The measurement results of both vehicles with stated iterations are given in Table 3.3.

Table 4.3 : Steering wheel vibration velocity (mm/s).

Velocity (mm/s)	Vehicle A with base mounts	Vehicle A with B mounts	Vehicle A with former level mounts	Vehicle B with base mounts	Vehicle B with A mounts
X	14,2	10,6	8,5	3,9	14,8
Y	4,8	4,7	1,7	1,2	1,5
Z	8,2	6,3	6,5	2,8	7,1
RSS	17,1	13,2	10,8	5,0	16,5

According to CAE results powerplant rigid body roll mode is increased with stiffening the rear engine mounts due to engine block failure. By using latest level mounts, powerplant rigid body roll mode increases. CAE results showed that powerplant rigid body roll mode increased from 16,4 Hz to 27,5 Hz with new engine mounts which couples with idle engine firing order (27,5 Hz). Roll mode is the most significant mode of powerplant because of being the most dominant mode caused by combustion.

In order to see the powerplant rigid body roll mode difference between vehicles A and B modal testing was conducted with base engine mounts. Results show that vehicle B, which has lower vibration levels, has lower roll mode frequency than vehicle A.

Vehicle A roll mode of 24,4 Hz -while Vehicle B roll mode is 19,7 Hz- is close to engine firing order which is one of the root causes of the high steering wheel vibration due to low modal separation of powerplant rigid body roll mode frequency and idle firing order frequency (27,5 Hz).

In order to isolate powerplant rigid body roll mode, at least 10 Hz separation from idle frequency required. This can be achieved by decreasing mount stiffness value or by changing idle engine speed.

Steering column adjustment mechanism and steering column attachment resonance frequency were investigated one each as a path for transmitting source vibrations to the steering column.

Since steering column adjustment mechanism can also be a path for transmitting source vibrations from instrument panel cross-car beam to steering wheel column, vibration levels were investigated when the adjustment mechanism is on and off position. According to the measurements, it had been identified that releasing lock mechanism has a remarkable effect on vibration levels. Comparisons of measurement results for locked and unlocked positions are given in Table 3.4.

Table 4.4 : Comparison of steering wheel vibration adjustment mechanism locked and unlocked.

	Steering Wheel Vibration Velocity - RSS (mm/s)	
	Locked	Unlocked
Vehicle A Base Condition	17,1	9,1
Vehicle B Base Condition	5,0	4,4

According to CAE analysis results, first mode of steering column is 24,3 Hz which is close to idle firing frequency (27,5 Hz) resulting poor idle vibration performance due to low attachment stiffness. Modal test was performed on instrument panel cross-car beam and steering column to identify if the modal testing results are correlated with CAE results. Modal testing results show correlation with CAE.

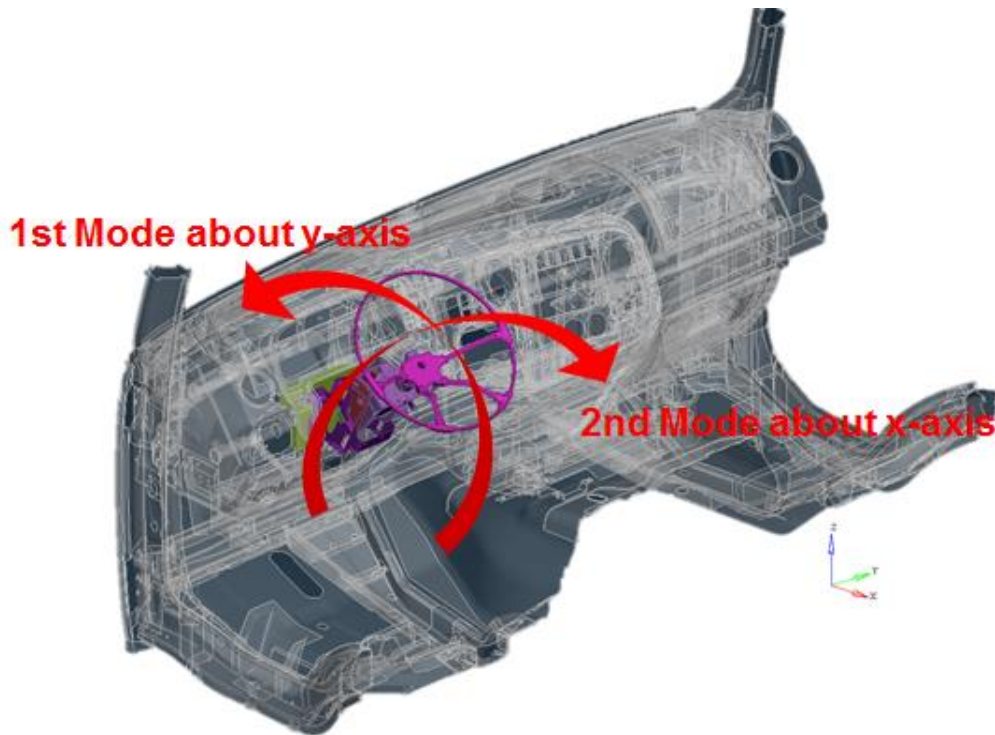


Figure 4.2 : Directions of first and second mode of the steering column.

Modal testing results for steering column are given in Table 3.5. 23,4 Hz and 26,4 Hz are too close to the firing frequency which is another root cause of the issue.

Table 4.5 : HXXX Steering column modes.

	CAE Results	Test Results
1st Mode	24,3 Hz	23,4 Hz
2nd Mode	31,9 Hz	26,4 Hz
3rd Mode	32,9 Hz	32,2 Hz

Instrument panel cross car beam and steering column stiffness should be increased to achieve higher mode frequency and sufficient isolation – target was to achieve 35 Hz first mode frequency. To increase first mode of the steering column, some modifications on steering column had been introduced. Lower side bolt connections to restrict the motion in z direction was added to the steering column (shown in Figure 3.4 as 1 and 2). To increase the stiffness of the cross car beam steering column connection, existing L-shaped bracket had been removed and instead of it, two reinforcement brackets was added. Additionally two more brackets (shown in Figure 3.4 as 3 and 4) were proposed to gain more stiffness to the steering column, however these brackets had been deleted since it has been later found out that these brackets worsen the steering wheel vibration.

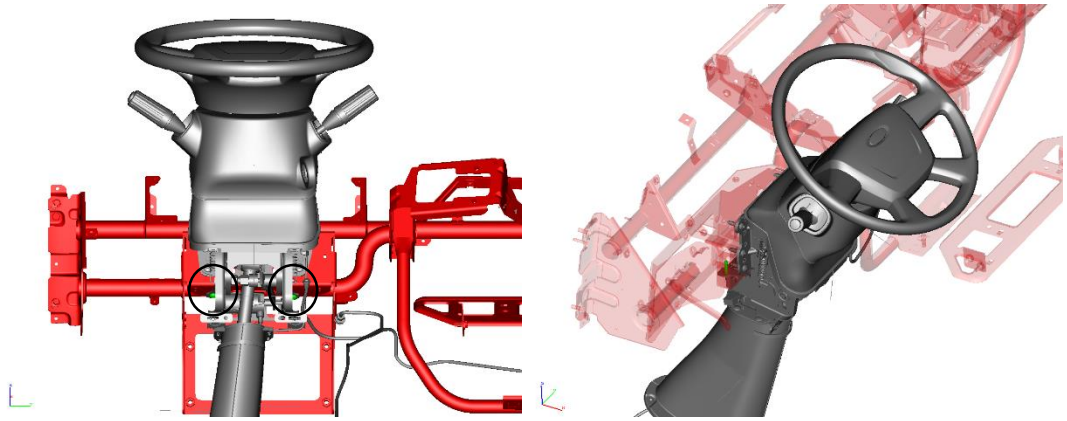


Figure 4.3 : Introduced steering column lower side bolt connections.

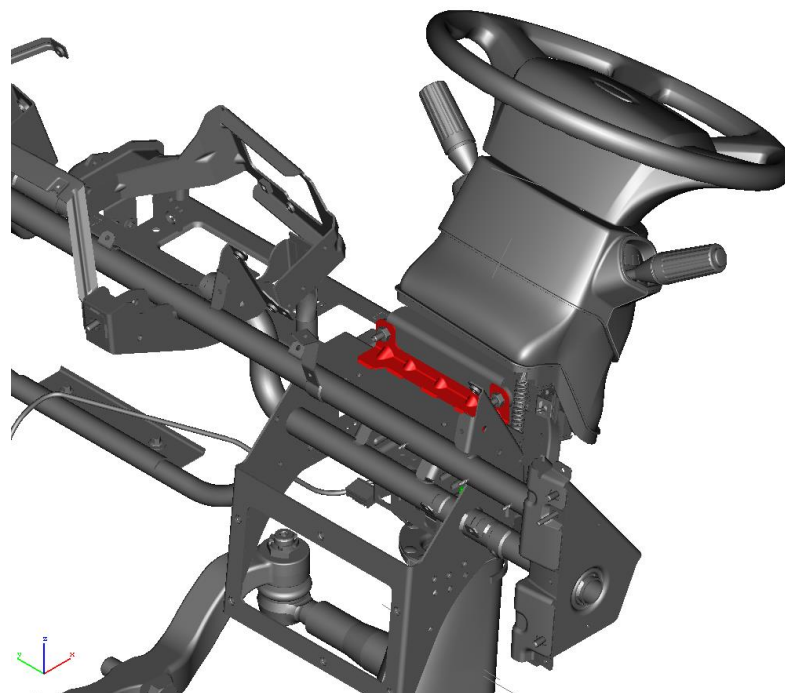
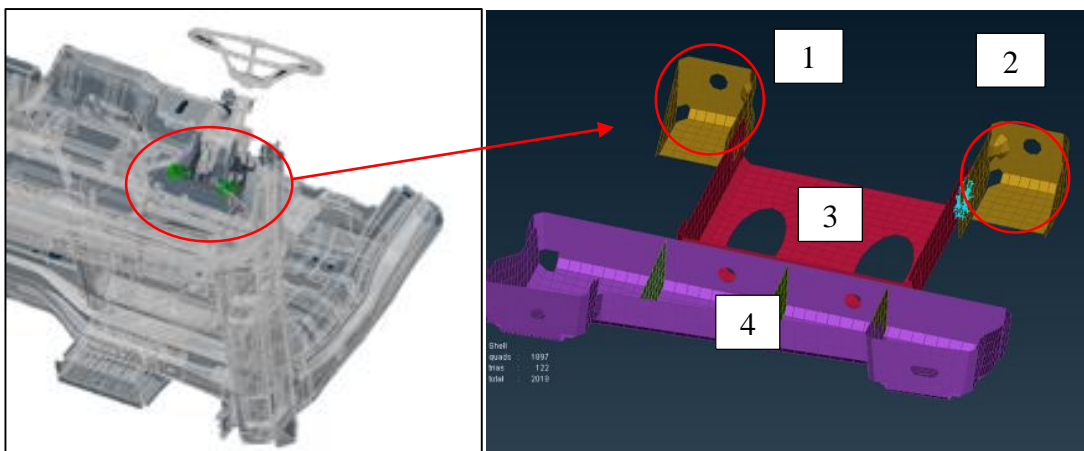


Figure 4.4 : Steering column – cross car beam connection reinforcements added (above) instead of the L-shaped bracket (bottom).

5. EXPERIMENTAL MODAL ANALYSIS OF HXXX STEERING WHEEL

With the next cycle action of HXXX program, a modified steering column was introduced to the program (see Chapter 3). To obtain the steering wheel and column dynamic behaviour change after the modifications on the steering column, modal tests on the steering wheel and column had been reperformed on a latest level prototype vehicle. Two modal test had been performed on steering wheel and column – without and with the steering column lower side bolt connections – to see the effect of the bolts on modal parameters. Newly introduced reinforcement brackets (1 and 2) were mounted on the vehicle before the test.

5.1 Test Instrumentation, Preperation and Setup

To obtain modal parameters of the steering wheel and steering column, two modal tests were performed with an impact hammer on HXXX. First test performed on the steering wheel as mounted to the cab and the second test performed on only the steering wheel as detached from the cab (free-free condition). The aim of performing modal analysis on steering wheel free free conditions was to use the test results to correlate the CAE model of the steering wheel.

The measurements for the modal analysis were performed using the Siemens LMS SCADAS multi channel analyzer system as shown in Figure 4.1.

Four Brüel&Kjær accelerometers, two different sized PCB Piezotronics impulse force hammer, Siemens LMS Test Lab 13A SL1 as data acquisitor and processor software were used for modal impact testing.

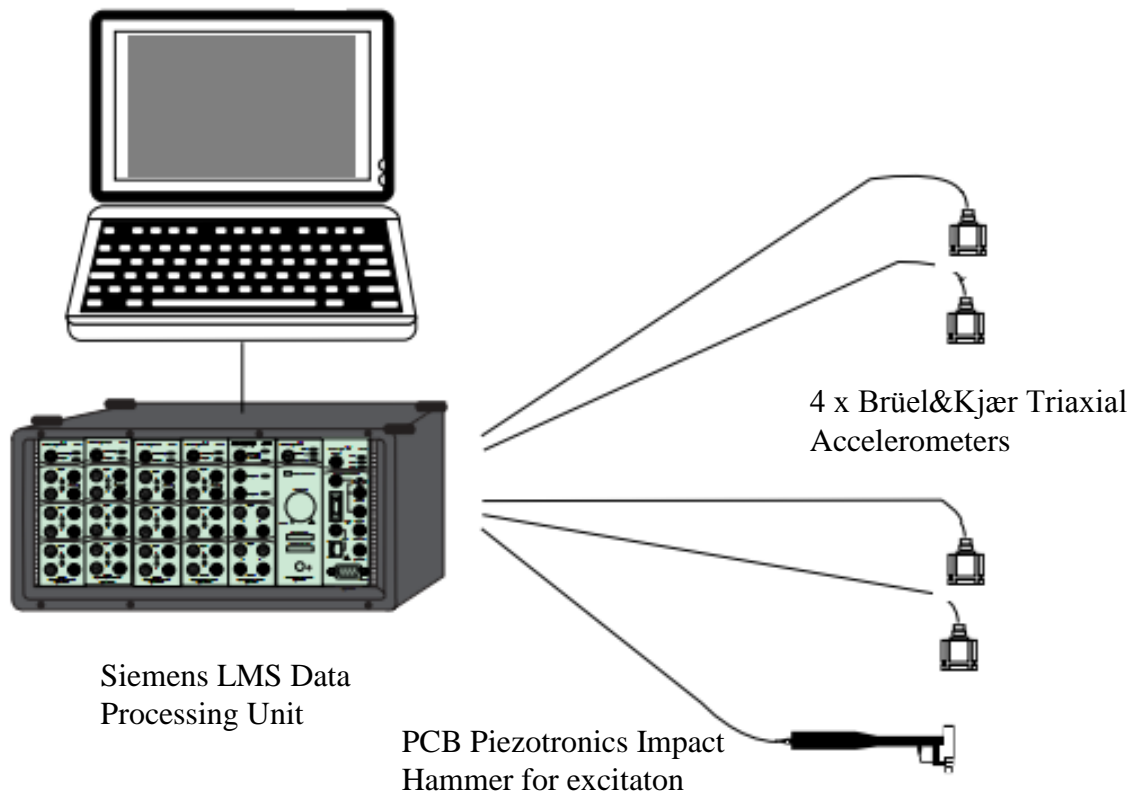


Figure 5.1 : Test setup plan for steering wheel modal testing.

Prototype vehicle had been updated with the latest level parts. Old L-shaped bracket was removed and proposed steering column cross car beam connection reinforcements attached before the test.

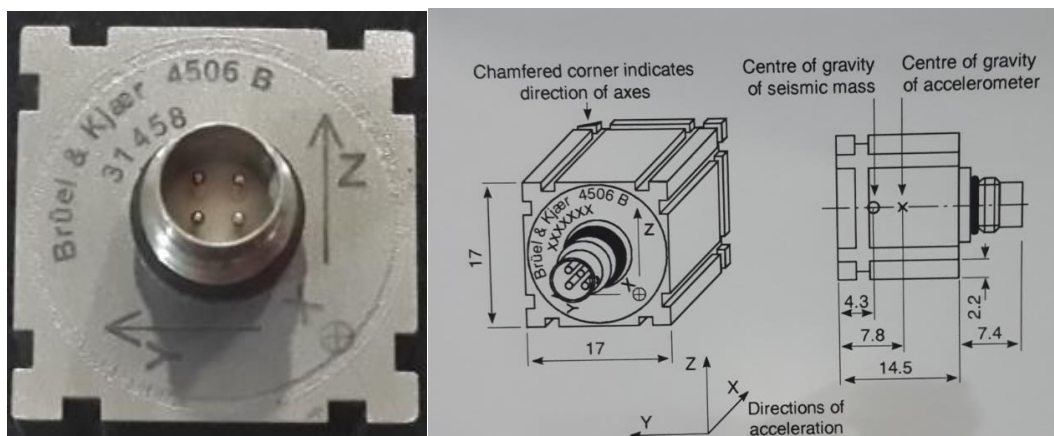


Figure 5.2 : Brüel&Kjær triaxial accelerometer.

Table 5.1 : Specification and calibration chart of the accelerometers.

Accelerometer Specifications	Sensor #31455	Sensor #31456	Sensor #31457	Sensor #31458
Manufacturer	Brüel&Kjær	Brüel&Kjær	Brüel&Kjær	Brüel&Kjær
Model	4506 B	4506 B	4506 B	4506 B
Type	Triaxial	Triaxial	Triaxial	Triaxial
Reference Sensitivity - X (mV/g)	97,9	97,3	94,85	94,48
Reference Sensitivity - Y (mV/g)	92,57	94,18	91,52	96,96
Reference Sensitivity - Z (mV/g)	94,14	98,56	92,26	95,46
Frequency Range - X (Hz)	0,3 - 5,5k	0,3 - 5,5k	0,3 - 5,5k	0,3 - 5,5k
Frequency Range - Y (Hz)	0,6 - 3k	0,6 - 3k	0,6 - 3k	0,6 - 3k
Frequency Range - Z (Hz)	0,6 - 3k	0,6 - 3k	0,6 - 3k	0,6 - 3k
Mounted Resonance Frequency - X (kHz)	18	18	18	18
Mounted Resonance Frequency - Y (kHz)	9,5	9,5	9,5	9,5
Mounted Resonance Frequency - Z (kHz)	9,5	9,5	9,5	9,5
Measuring Range	+/-700 m/s ² peak	+/-700 m/s ² peak	+/-700 m/s ² peak	+/-700 m/s ² peak

Two hammers were used in the tests since the hammer used for the detached steering wheel test (referred to as hammer no #2 hereafter), was not sufficient to excite the accelerometers which were placed on the steering column and mounting bracket while performing the test steering wheel is on the vehicle. Specifications of the accelerometers and hammers are given in Tables 4.1 and 4.2, respectively.



Figure 5.3 : Impact hammer used for first test (hammer #1) which was performed on HXXX steering wheel as attached to cab.



Figure 5.4 : Impact hammer used for the second test (hammer #2).

Table 5.2 : Specifications of the impact hammers used for the modal test.

Hammer Specifications	No #1	No #2
Model No	086C41 (084A61 – soft plastic brown tip)	086D05
Manufacturer	PCB	PCB
Sensitivity ($\pm 15\%$)	0.23 mV/N	0.23 mV/N
Measurement Range	$\pm 22,000$ N pk	± 22240 N pk

The measurements for the modal analysis were performed using the LMS multi-analyzer system which is shown in Figure 4.5. LMS Test Lab Structures, a dedicated application software package, was used for the measurements and data validation. LMS Test Lab Structures Impact Testing and Modal Analysis modules were used to support the generation and import of geometry, definition of measurement sequences on the various points and directions (DOFs), and subsequent transfer/export of DOF-labelled measurement data.



Figure 5.5 : Measurement and data processing equipment.

5.2 Modal Test of Steering Wheel and Column on Vehicle

Eight accelerometers on steering wheel and two accelerometers on steering column were placed on mounting clips which were fastened by glue on the measurement locations. Since there was four accelerometers, test had been completed in three turns. The aim of the measurements was to determine the lower modes considering idle frequency, thus 0 – 160 Hz frequency range was of interest (0 - 320 Hz range was set in the LMS software as the frequency range to obtain reliable results between the interested frequency range before damping be effective on the results).

Accelerometers on the steering wheel positioned at twelve o'clock position (top of the wheel), on spoke and wheel intersections, points between spokes and wheel top (one at ten o'clock and one at two o'clock position) and center of the hub. Two accelerometers were placed on steering column. Accelerometer locations are shown in Figures 4.7, 4.8, 4.9 and 4.10.



Figure 5.6 : HXXX steering wheel on vehicle.

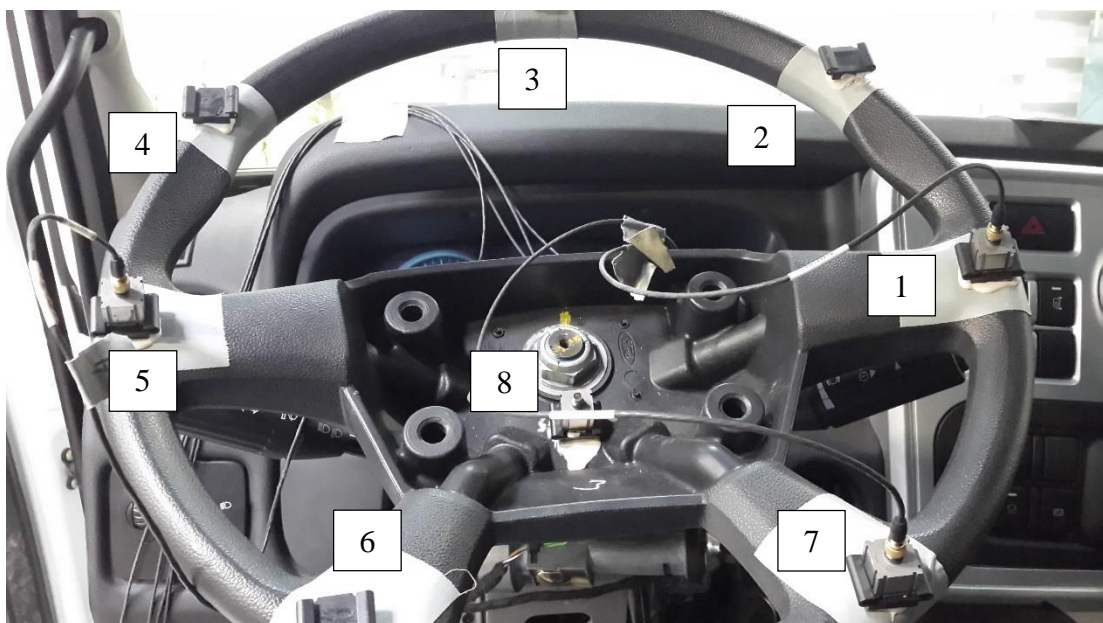


Figure 5.7 : Accelerometer locations on steering wheel.

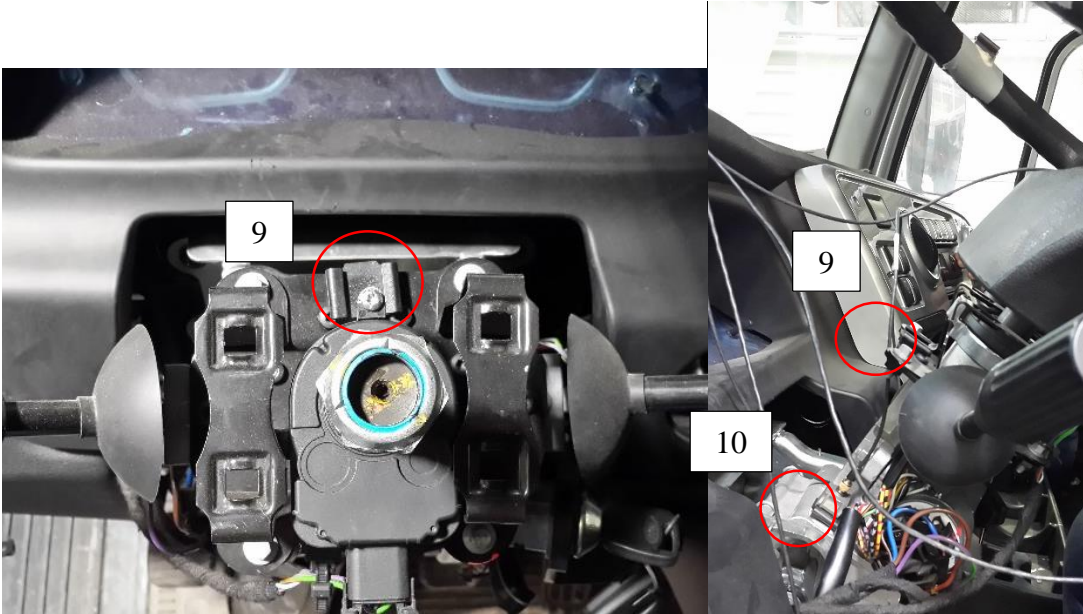


Figure 5.8 : Accelerometers #9 and #10 located on steering column.

Impact was applied to the steering wheel rim 3 o'clock position, Point 1, and measurements were taken from Point 1 to 10. Impact applied perpendicular (in the direction of Z) and horizontal (in the direction of Y) to the steering wheel rim, respectively as shown in Fig. 4.9 a and b. Since there was 4 accelerometers, measurements taken from points 1, 2, 3, 4 firstly, then the accelerometers were removed and mounted to points 5, 6, 7 and 8 in the second turn, and same process repeated for points 9 and 10.

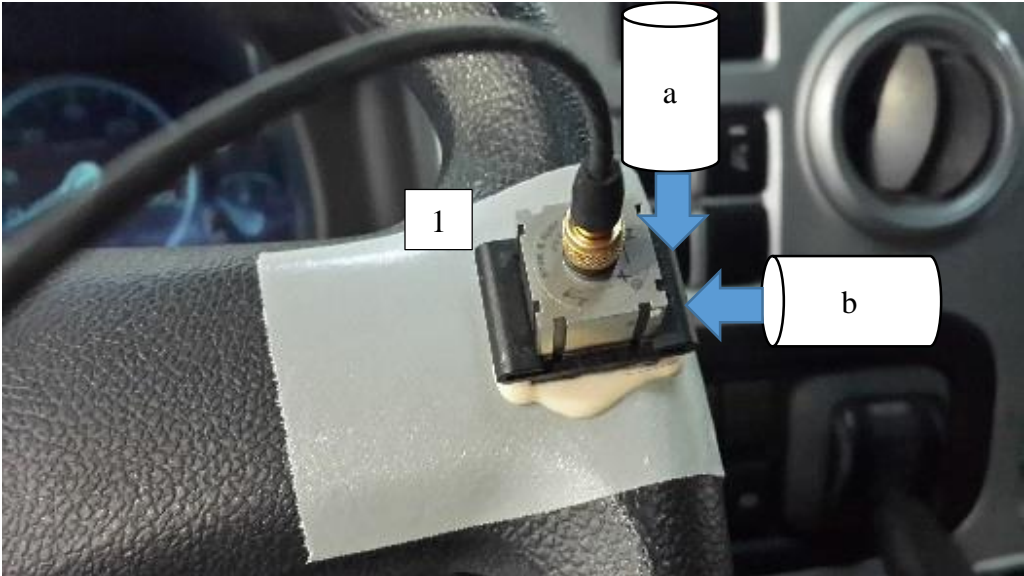


Figure 5.9 : Accelerometer positioning on the steering wheel, Point-1 (excitation point).

5.3 Modal Test of Steering Wheel Free-Free Condition

Steering wheel detached from the test vehicle and tied to a rope and hanged down to isolate the test object from the environment and demonstrate free-free boundary conditions. The main objective aimed performing steering wheel free free test was to use the test results for the correlation of the steering wheel finite element model.

Force was applied to Point 1 (3 o'clock position) with the smaller impact hammer to excite the steering wheel. Force was applied to $-X$ and $+Y$ direction.

There was eight measurement points on the steering wheel: 1 accelerometer on steering top of the rim (12 o'clock), 4 accelerometers on spoke and rim intersections, 2 accelerometers on unsupported section on the rim which is between top of the rim and spokes (about 3 o'clock and 10 o'clock) and 1 accelerometer on just below the wheel hub. Frequency responses between 0 – 320 Hz was area of concern, thus 0 – 640 Hz frequency range set in the LMS software to avoid damping effect on frequency responses.

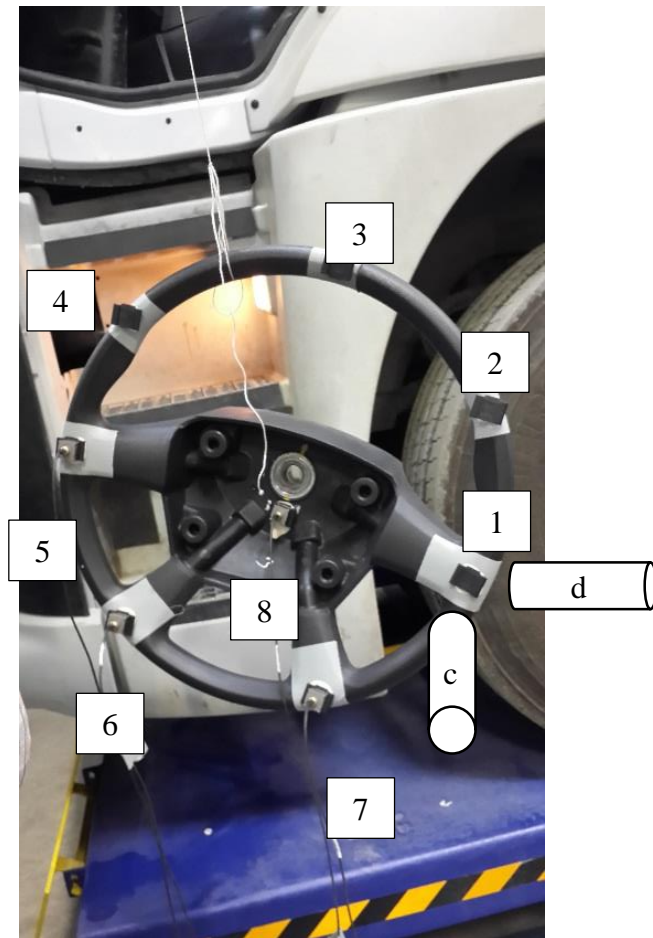


Figure 5.10 : Impact and measurement points on the steering wheel.

5.4 Results of the Experimental Modal Analysis

Accuracy of the results had been checked by tracking the resultant diagrams, mainly coherence diagram during the test after each measurement. From the diagrams obtained from the measurements, it was ensured that;

- Frequency response function have peaks at the frequencies corresponding to the natural frequencies of the test object
- Between two natural frequencies (peaks), there is an anti-resonance point which seems like an inverse peak in the diagram
- In the coherence diagram, there is breakdowns where corresponds to anti-resonance regions
- For all the regions except anti-resonance regions, coherence function is equal to 1

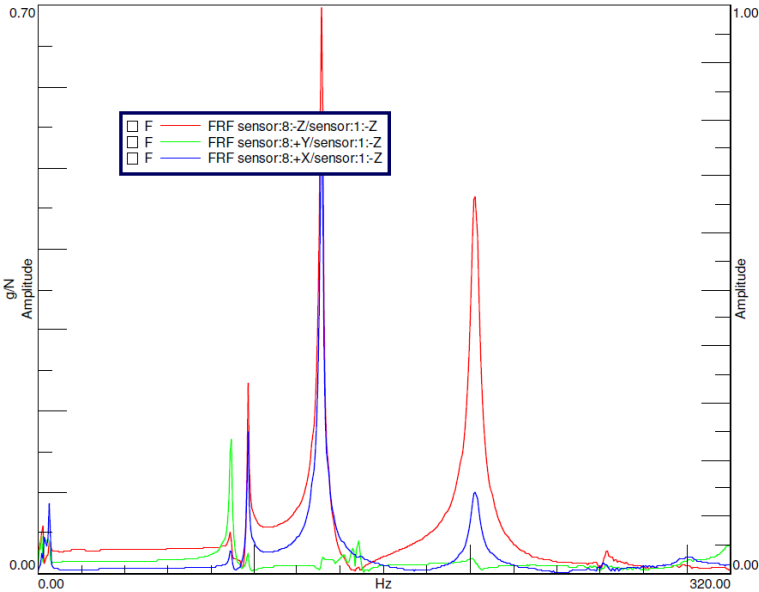


Figure 5.11 : Example of frequency response function (accelerance).

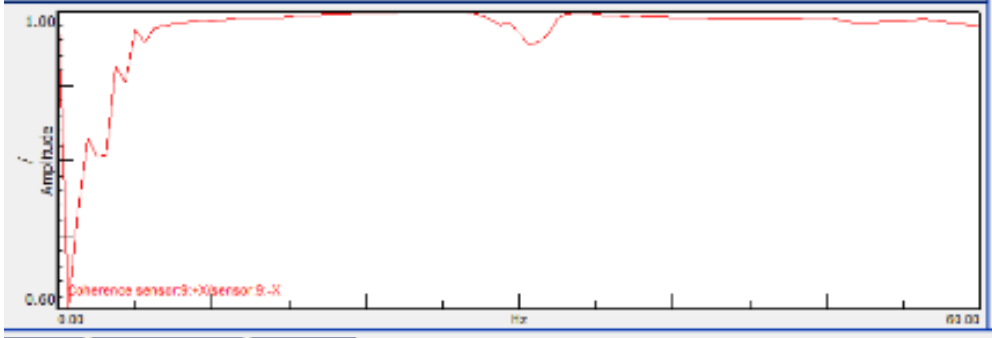


Figure 5.12 : Coherence function diagram.

Natural frequencies and modal shapes of steering wheel and column were obtained from frequency response function stabilization diagrams. First three modes of the steering wheel and column and steering wheel free free are given in Table 4.3 and Figure 4.13, respectively.

Table 5.3 : Steering wheel and column modes.

	W/O bolts	With bolts	SW Free - Free
1st mode	25,5 Hz	27,9 Hz	96,3 Hz
2nd mode	27,8 Hz	29,4 Hz	126,5 Hz
3rd mode	53,6 Hz	31,6 Hz	150,2 Hz

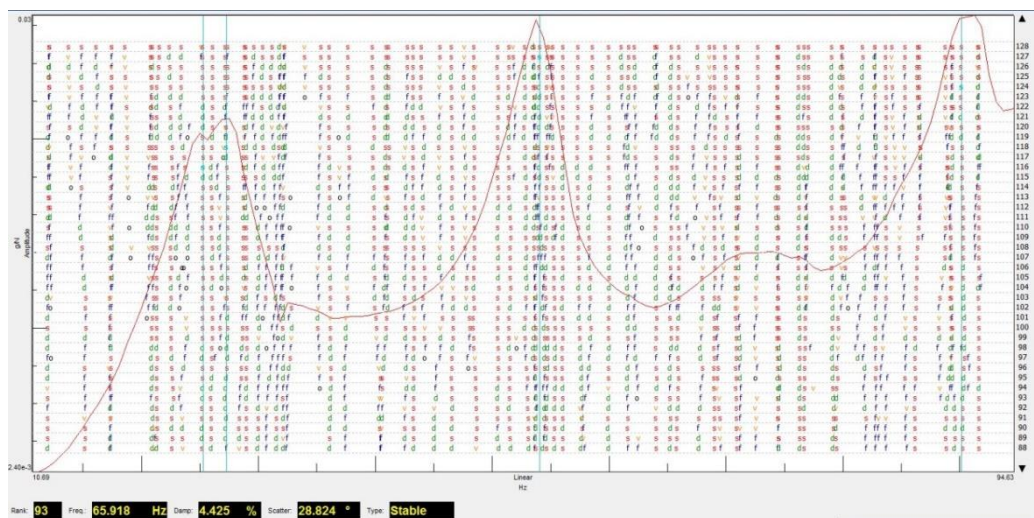


Figure 5.13 : FRF stabilization diagram.

Table 5.4 : Modes directions of the steering wheel and column.

	Free Free	On Vehicle
Vertical Column Mode	-	25,5 Hz
Horizontal Column Mode	-	-
Vertical Steering Wheel Top Mode	96,3 Hz	27,8 Hz
Horizontal Steering Wheel Top Mode	126,5 Hz	53,6 Hz

5. FINITE ELEMENT MODAL ANALYSIS OF HXXX STEERING WHEEL AND COLUMN

For dynamic structural analysis, the finite element model of the cab of HXXX with all components were used. The three dimensional model of the cab and steering system was built using CATIA V5 software, exported as STP format, and it is imported into ANSA software. ANSA and μ ETA, the pre-and post-processing package of BETA CAE Systems was used for modelling and post processing, respectively. Before building the finite element model, free surface of the model is checked to ensure all the surfaces are closed. Finite element analysis was performed using NASTRAN.

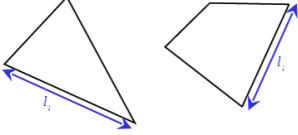
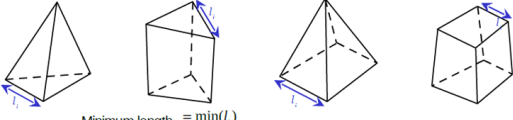
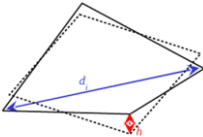
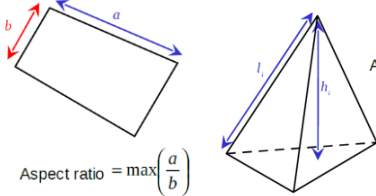
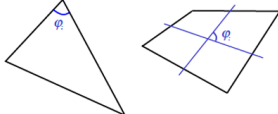
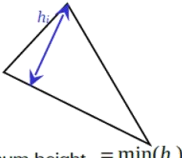
5.1 Finite Element Model of Trimmed Body

CAE model of the trimmed body was generated in ANSA. A trimmed body structure may be thought of as a vehicle without the chassis (frame, suspension, brakes) and powertrain sub-systems. When all the closures (door, hood, decklid) and other sub-systems (steering column, seats) and trim items (carpeting etc.) are removed from trimmed body, the resulting structure is called the "body-in-prime" (or the "body-in-white" with glass). A FE trimmed body model is created by 'trimming up' a BIP (Body-In-Prime) model with system models such as closures, seats, IP (instrumental panel) assembly (including steering column, steering wheel, cross car beam), bolted-on sub-frames, and non-structural trim items (heater module, and carpets etc.). BIP and trimmed body play an important role in determining the dynamic characteristics of the vehicle.

Trimmed body FEM model consists of 1311966 shell elements in total (959924 quads, 352042 trias) and 1272711 volume element in total (1233609 tetras, 1674 pentas and 37428 hexas).

The meshing parameters and quality criteria were imported into ANSA to ensure that the generated mesh fulfill the prescribed quality criteria. Meshing and quality criteria are shown at Table 5.1.

Figure 5.1 : Quality criteria definitions of shell and solid mesh.

			95% of elements	100% of elements	
1	Minimum Element Length	 <p>Minimum length = $\min(l_i)$ Maximum length = $\max(l_i)$</p>		5 mm	
2	Maximum Element Length	 <p>Minimum length = $\min(l_i)$ Maximum length = $\max(l_i)$</p>	< 18 mm	< 25 mm	
3	Mean Element Length			12	
4	Warpage	 <p>Warping = $\max\left(\frac{h}{(d_1 + d_2)/2}\right)$</p>	< 10°	< 15°	
5	Aspect Ratio	 <p>Aspect ratio = $\max\left(\frac{a}{b}\right)$ Aspect = $\frac{\max(l_i)}{\min(h_i)}$</p>	< 3	< 5	
6	Skewness	 <p>Skew = $\min(\phi_i)$</p>		<15	
7	Minimum Height (tria)	 <p>Minimum height = $\min(h_i)$</p>	5 mm	5 mm	
8	% trias		<13%	<13%	
9	Jacobian	The reported distortion is calculated as the ratio of the smallest value over the largers. A reported distortion value of 1 corresponds to the ideally shaped element. Negative distortion values correspond to concave elements. First order triangles always have a value of 1.		> 0,7	> 0,5

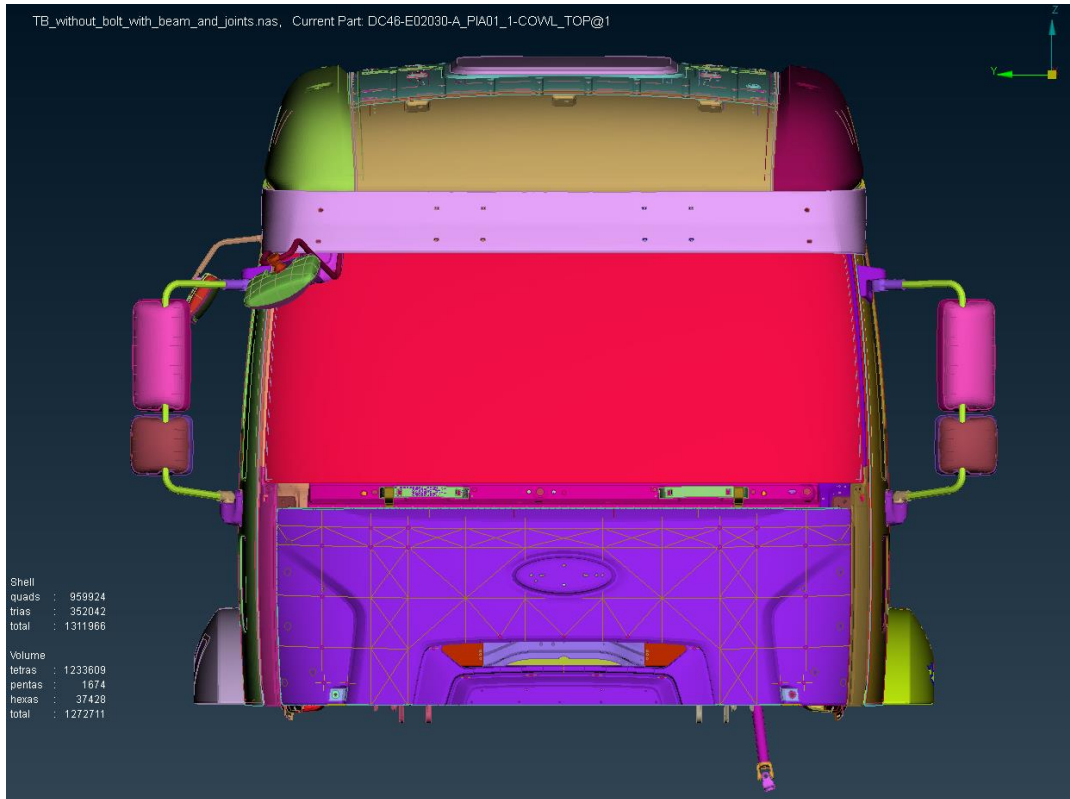


Figure 5.2 : Finite element model of the cab.

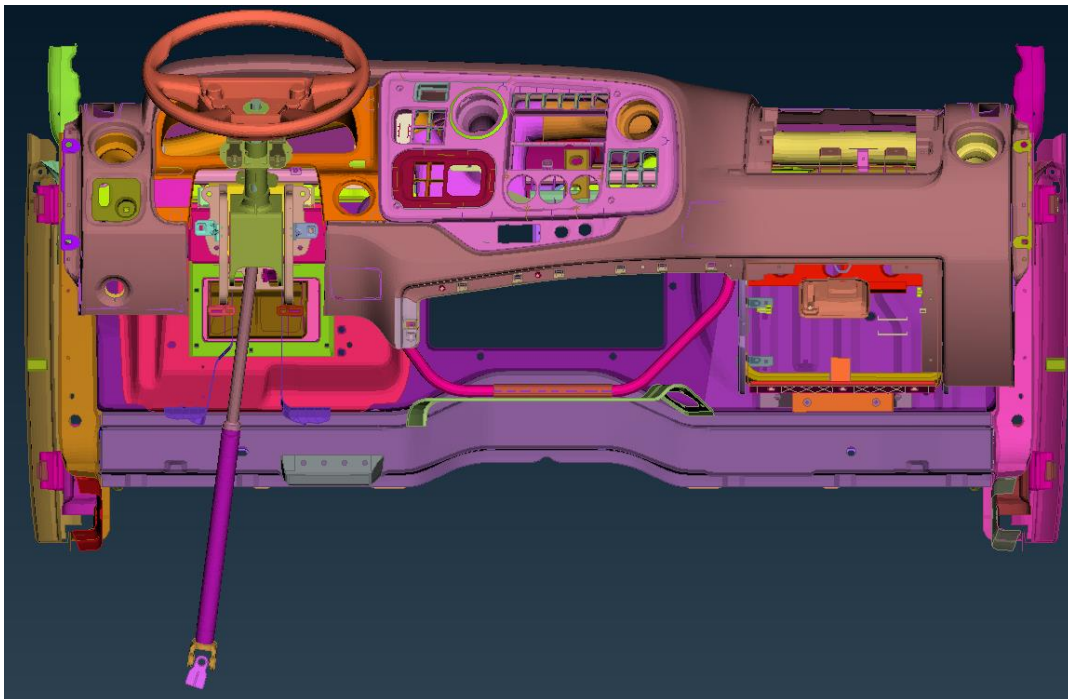


Figure 5.3 : Display model.

5.2 Finite Element Model of the Steering Wheel

Steering wheel assembly consists of armature and rim, urethane cover, airbag bracket, airbag, spoke cover and stub shaft. Stub shaft and air bag bracket was not included in the model since the tested steering wheel has no stub shaft and air bag bracket on it while testing.

HXXX steering wheel FE model consists of total number of 34891 shell and 130656 solid elements. Armature with rim (as on casting parts) and polyurethane covering of the rim, spoke and the armature modeled with 3D CTETRA elements with 3,0 mm average element size. On the top of the solid mesh, meshed with 2D CTRIA3 shell elements which has a thickness of 0,05 mm. Common grids between steering wheel and wrapping foams and RBE2 for rigid connections such as bolts or screws were used. Important features such as beads and ribs and all holes with their diameters equal to or greater than 5 mm has been included in the model. The model quality is considered acceptable when it meets the general FE mesh quality requirements.

Steering wheel assembly constrained as it is hanged from the rim using single point constraint to restrict z translation direction from the same point (1 o'clock) which steering wheel hanged from during the modal testing.

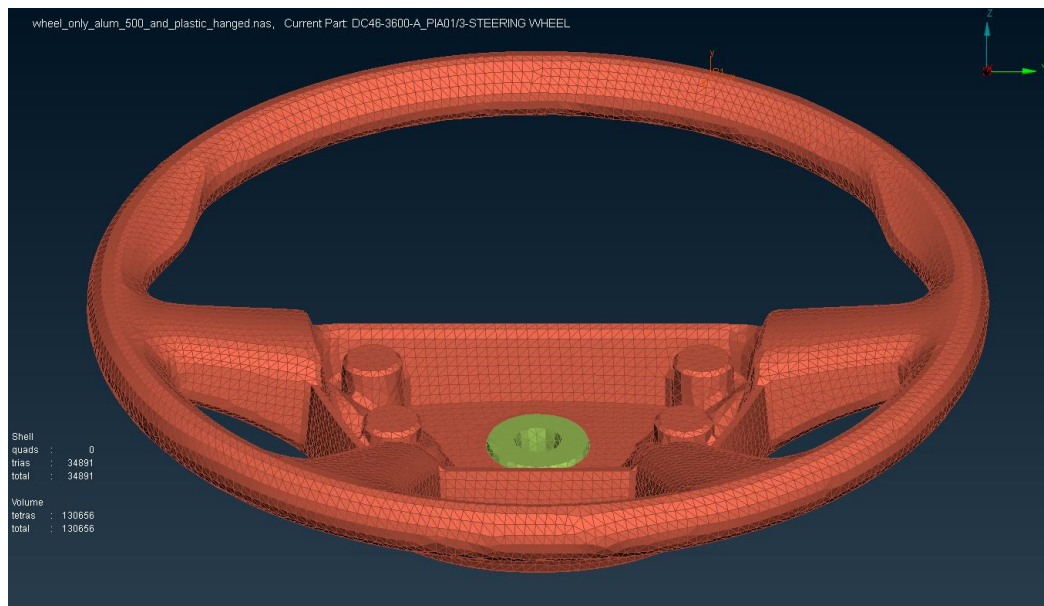


Figure 5.4 : Steering wheel assembly finite element model.

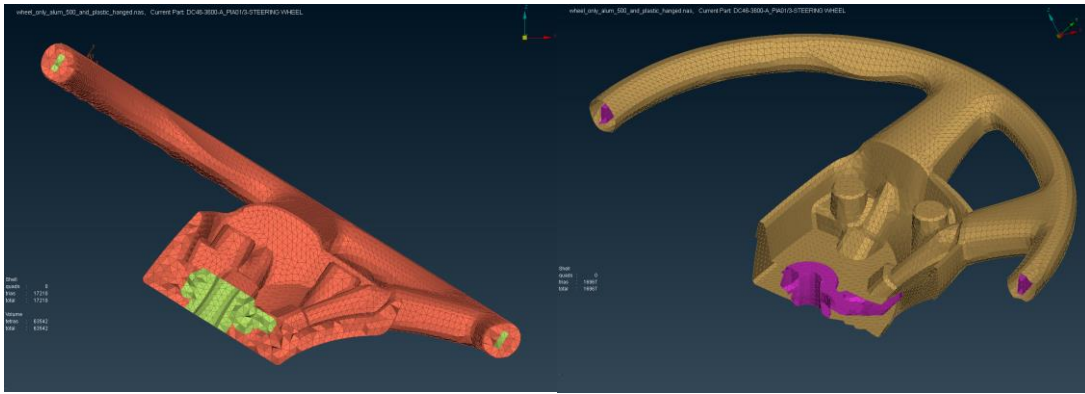


Figure 5.5 : Steering wheel solid mesh (left) and shell mesh (right).

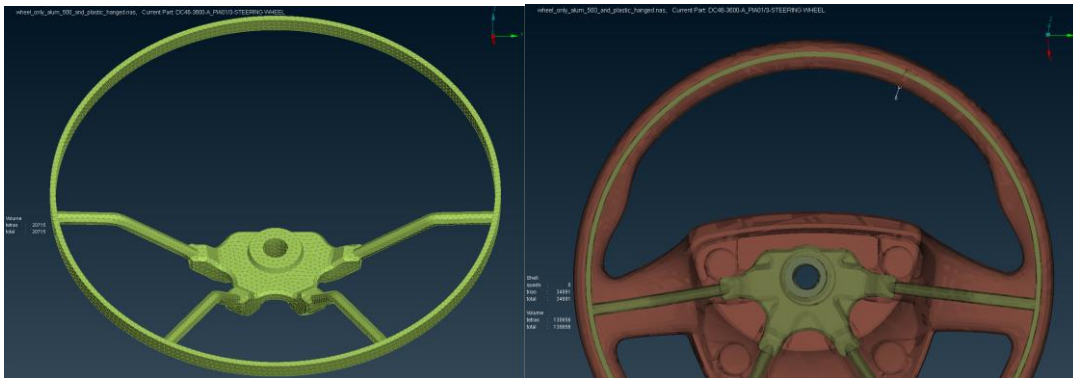


Figure 5.6 : Steering wheel insert model (left), steering wheel single point constraint point (right).

Aluminum material properties were assigned to the armature. Polyurethane material properties were assigned to the rim and hub cover. Total mass of the steering wheel assembly is 3,4 kg which is the exact weight of the steering wheel measured during the test.

5.3 Results of the Finite Element Analysis

Finite element analysis has been performed initially on trimmed body to obtain steering wheel and column modes. Several modifications and improvements had been done on the model such as deletion of the L-shape brakets and addition of two reinforcement brackets instead, addition of steering lower shaft model and steering wheel model modification to get more corelated results with the experimental modal anlaysis.

Also finite element analysis has been performed on only steering wheel before and after steering wheel model improvement. Improvements has been done on the steering

wheel model by the help of the modal test results performed on free-free steering wheel assembly in free-free condition. Iterations has been done till the modal frequencies of the steering wheel converge to the test results.

Also finite element analysis has been reperformed with several iterations such as addition of the bolts which was proposed to improve steering wheel vibration.

5.3.1 Finite element analysis of the trimmed body

Trimmed body finite element model was submitted to the super computer and finite element analysis has been performed in NASTRAN by applying free free boundary conditions. Bolts were removed from the trimmed body model for the first analysis. A second analysis has been performed with the bolts added to the model to get an estimation of the modal behavior change of the steering system with the proposed bolts which will restrict z movement of the steering column assembly.

Output file was processed through MetaPost. There are seven rigid body modes, the first six modes are rigid body modes of the steering wheel and seventh mode is rotation of the steering column about its local axis. For trimmed body, there is an additional steering wheel nimble mode which is very close to 0 Hz (usually around 0,2 Hz). Additional rigid body modes usually are an indication of unconnected or mis-connected parts.

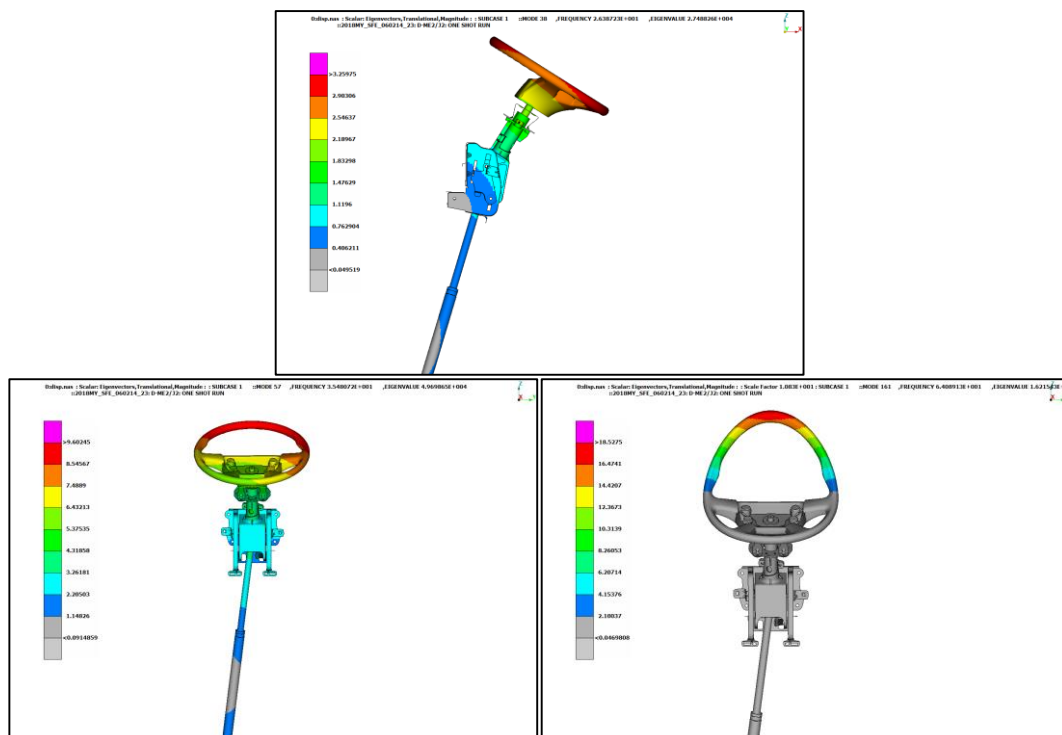


Figure 5.7 : Mode shapes of steering wheel and column without proposed bolts.

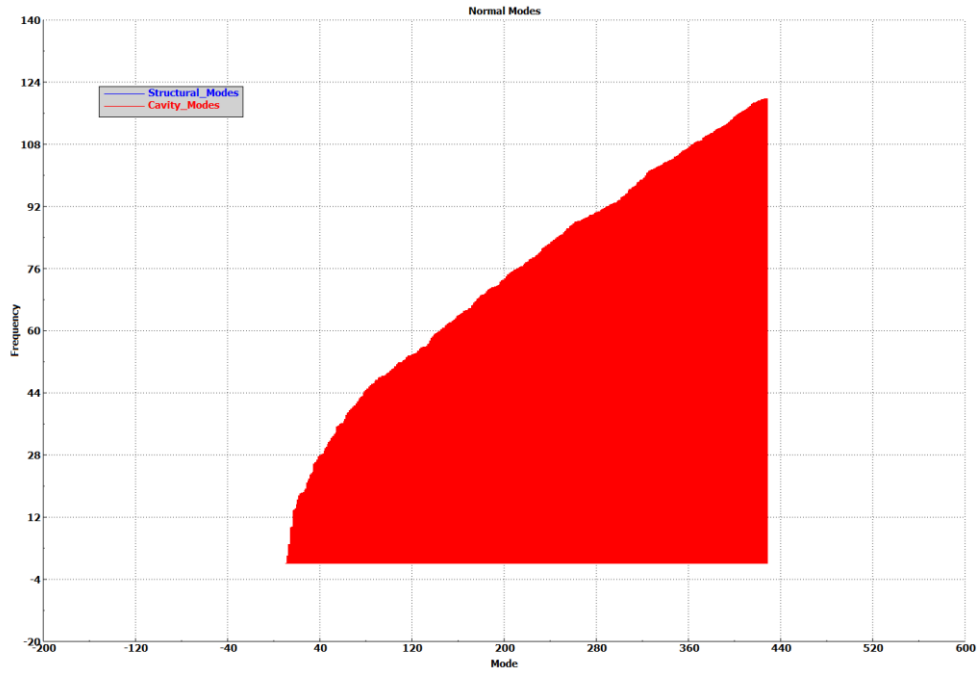
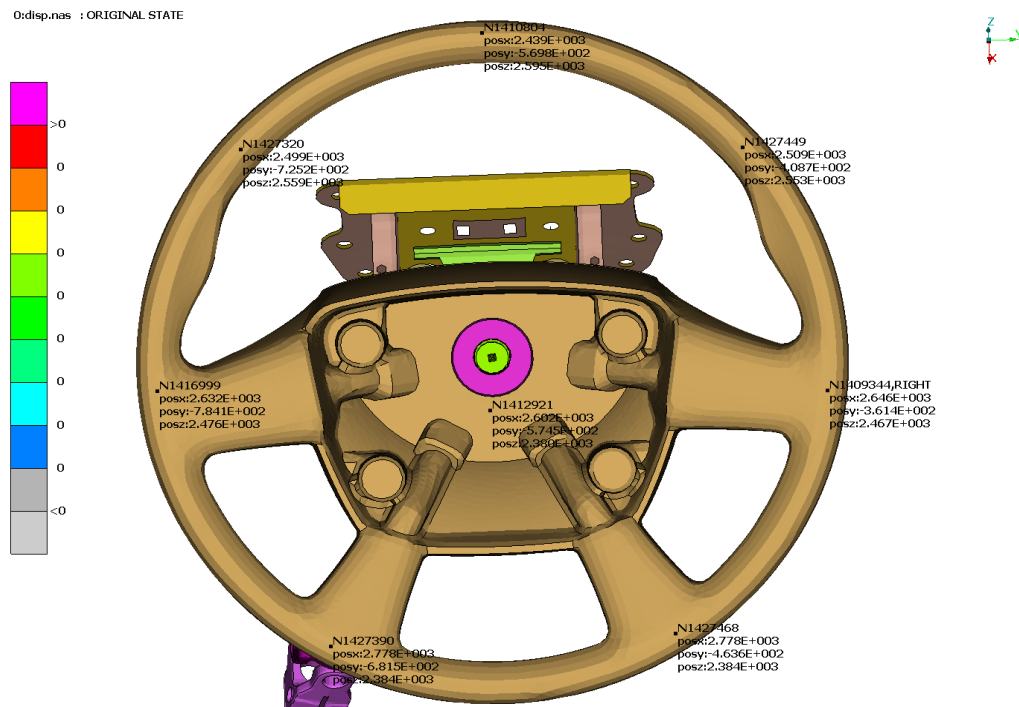


Figure 5.8 : Trimmed body frequency – mode diagram.

To obtain the steering wheel and column modes, measurement nodes were defined on the display model. Nodes around the region where measurements were taken from during the modal test on the steering wheel and column were picked on the model and response frequencies were collected.



0:disp.nas : ORIGINAL STATE

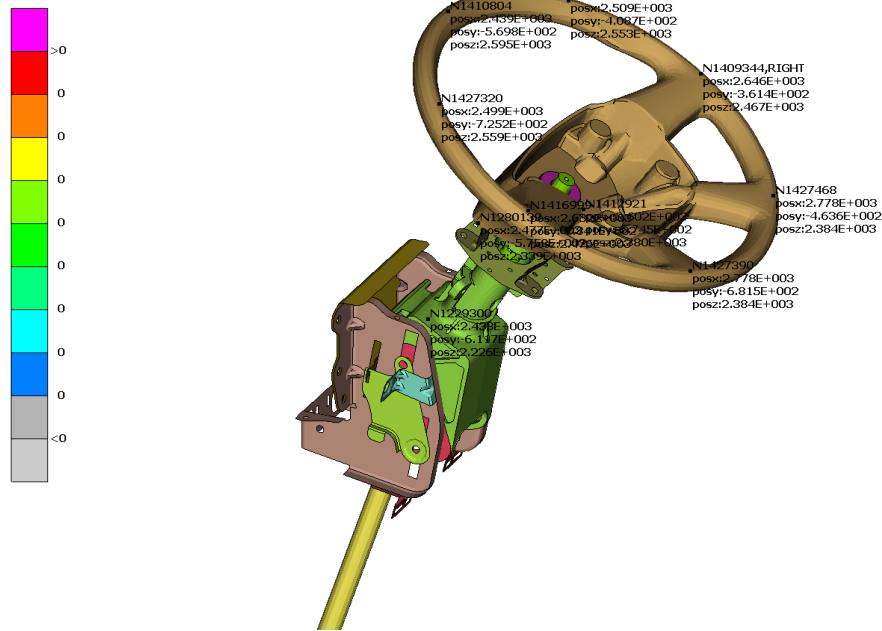


Figure 5.9 : Nodes selected to obtain the modal frequencies.

Table 5.1 : Steering wheel and column modes according to trimmed body CAE results.

		Vertical - Column mode	Horizontal - Column mode	Wheel top (x) mode	Wheel top (y) mode
Frequency	Without bolts	26,5 Hz	35,5 Hz	64 Hz	147 Hz
	With bolts	27,6 Hz	36,9 Hz	64,6 Hz	147 Hz

According to the finite element analysis results, first mode (vertical column mode) is correlated with the test results. However, correlation between finite element analysis and test results decreased with the following modes. Since the finite element model of the trimmed body consists of great number of parts, material assumptions, shell modelling of thin parts, shell thickness estimations and contact point assumptions can contribute to diverged results. All assumptins that have been made for material properties, shell thickness values, contact points must be rechecked and updated if required. If results compared with previous results, before steering column and reinforcement bracket change, vertical column mode increased with the introduced bolts and brackets. The steering column first mode is still very close to engine idle

firing frequency. First mode (vertical column mode) must be increased to achieve the target setted (35 Hz).

5.3.2 Finite element analysis of steering wheel in free-free condition

Normal mode analysis has been performed in NASTRAN of the steering wheel assembly from 0 to 320 Hz with the DOF 123456 non-constrained (free-free boundary conditions).

The first six modes are the steering wheel rigid body modes. Modal frequencies of the steering wheel assebly are obtined from Frequency – Mode chart given in Figure 5.10 and given in Table 5.2.

Finite element model of the steering wheel was improved before the analysis since analysis results before the model modification was not corelated with the test results. Rim and hub cover model was added to the previous model.

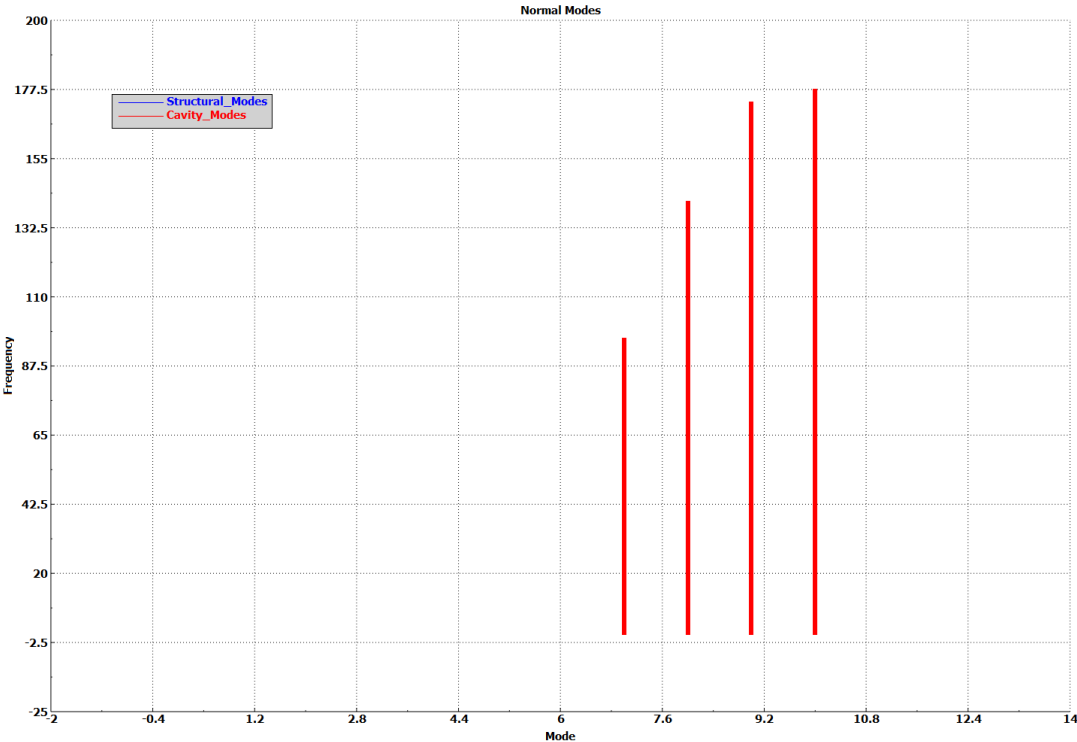


Figure 5.10 : Steering wheel frequency – mode diagram.

Table 5.2 : Natural frequencies of HXXX steering wheel in free – free condition.

Mode	Frequency (Previous SW FE Model)	Frequency (Improved SW Model)
1st	93,2 Hz	96,6 Hz
2nd	122,4 Hz	141,3 Hz
3rd	153,8 Hz	173,5 Hz

As seen from the results, a correlation between steering rim top vertical mode has been achieved steering wheel rim top lateral mode is not correlated with test.

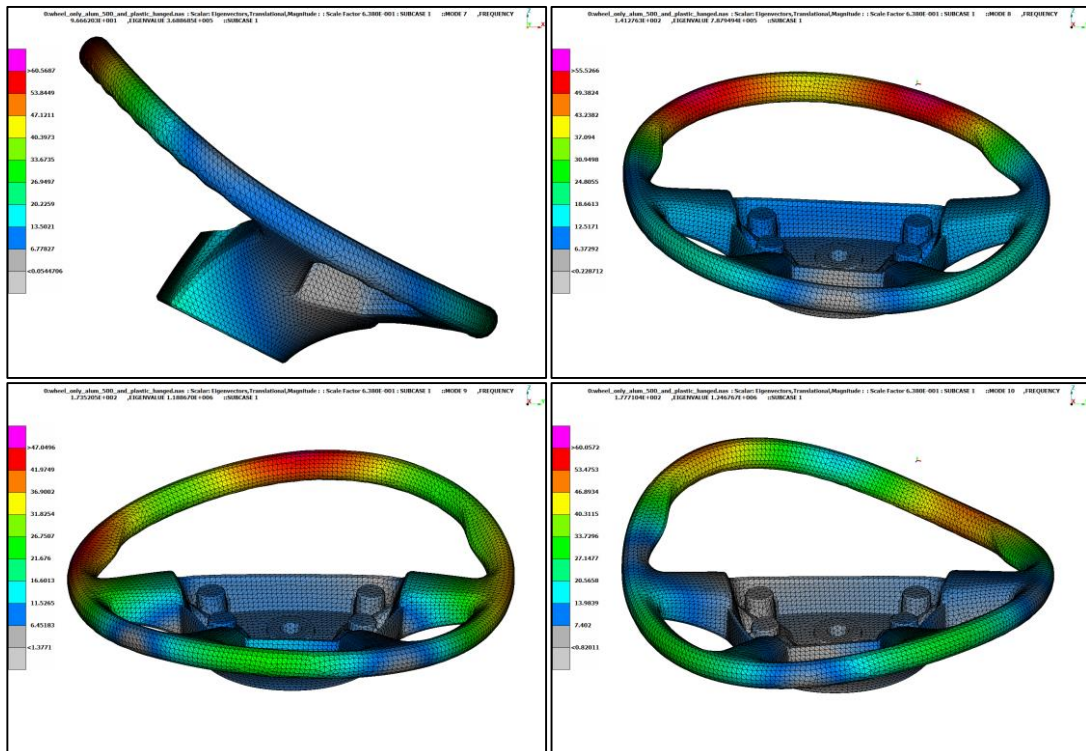


Figure 5.11 : Mode shapes of the steering wheel.

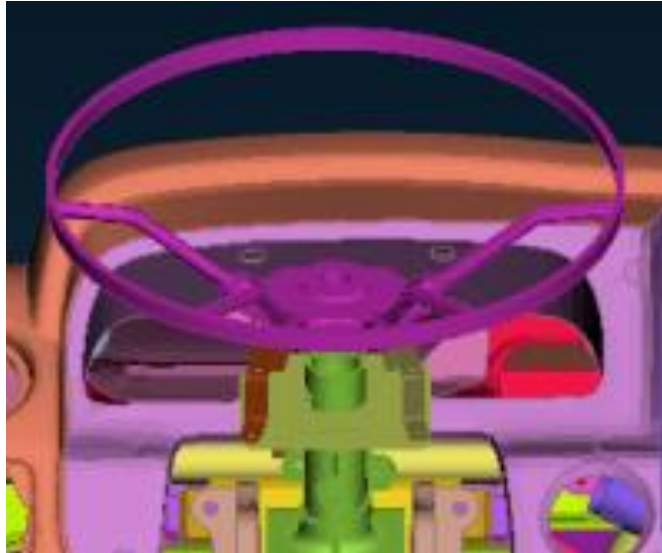


Figure 5.12 : Previous steering wheel FE model.

Table 5.3 : Comparison of experimental and finite element modal analysis

Steering Wheel Free - Free	Experimental Modal Analysis	Finite Element Analysis
1st Mode	96,3 Hz	96,6 Hz
2nd Mode	126,5 Hz	141,3 Hz
3rd Mode	150,2 Hz	173,5 Hz

Steering Wheel and Column	Experimental Modal Analysis	Finite Element Analysis
1st Mode	25,5 Hz	26,5 Hz
2nd Mode	27,8 Hz	35,5 Hz
3rd Mode	53,6 Hz	64 Hz

6. CONCLUSIONS AND RECOMMENDATIONS

In this study experimental modal analysis and finite element analysis had been performed on the steering wheel and column of HXXX. According to the finite element analysis results performed on free free steering wheel, first mode of the steering wheel is highly correlated with the test results. Correlation between experimental and FEA results has been achieved by steering wheel CAE model improvement. The second and third modes of the steering wheel are still not correlated with experimental modal analysis results. Even there is nearly any geometry simplifications applied on the CAE model, material property assumptions -especially considering the steering wheel rim exact material properties were unknown-, shell meshing of thin components, estimated shell thicknesses and contact point assumptions may have lead to uncorrelated results.

According to experimental modal analysis results, steering column vertical mode is 27,9 Hz which is still very close to the engine idle firing order frequency. Before column modification, vertical mode of the steering column was 23,4 Hz. 4,5 Hz increasement has been achieved but the target was above 35 Hz so design optimization must be performed on the brackets proposed. Steering column holder bracket must be extended as much as possible in vertical axis to increase the first mode of the steering column to restrict the vertical motion.

The implementation of the proposed bolts is verified by test and finite element analysis. The experiments and analysis has been performed with and without bolts. Comparisons of the measured and the predicted results indicate that the bolts increased the steering column vertical mode about 2,4 Hz.

Experimental modal analysis should have been repeated with a production line vehicle to obtain the most accurate modal behaviour of the steering system. Modifications of finite element model of the steering wheel and column required to get more correlated results.

REFERENCES

- [1] **Jeon H. B. (2010)**. Proposed Automobile Steering Wheel Test Method for Vibration, School of Engineering and Design Brunel University
- [2] **Szczotka M. (2011)**. Simulation and Optimization of the Steering Kickback Performance, *Journal of Theoretical and Applied Mechanics*, 49, 1, pp. 187-208.
- [3] **Kim B., Grenier G., Cerrato-Jay G. (2007)**. A Numerical and Experimental Study on Power Steering Shudder, SAE International
- [4] **Mangun D. A. (2006)**. Simulation and Characterization of Tire Nonuniformity Induced Steering Nibble Vibrations Through Integrated Subsystems Modeling, A Thesis Presented to the Graduate School of Clemson University, Master of Science, Mechanical Engineering
- [5] **Sugiyama A., Kurishige M. (2006)**. An EPS Control Strategy to Reduce Steering Vibration Associated with Disturbance from Road Wheels, SAE International
- [6] **Zhang L., Ning G., Yu Z. (2007)**. Brake Judder Induced Steering Wheel Vibration: Experiment, Simulation and Analysis, SAE International
- [7] **Matsunaga T. (2001)**. Analysis of Self-Excited Vibration in Hydraulic Power Steering System: Prevention Against Vibration by Supply Line, Toyota Central Research & Development Labs., Inc., Society of Automotive Engineers, Inc.
- [8] **Wang S., Shi W., Wu G., Nie S. (2013)**. Research and Improvement of Steering Wheel's Idle Shaking, SAE International
- [9] **Demers M.A. (2001)**. Steering Wheel Vibration Diagnosis, Ford Motor Co., Society of Automotive Engineers, Inc.
- [10] **Kim J. H., Jung S. G., Kim K. S.** An Investigation of the Steering Wheel Vibration and Its Reduction In Passenger Cars, Hyundai Motor Co., Ltd., Engineering Research Center
- [11] **Botti J., Venizelos G., Benkaza N.** Optimization of Power Steering Systems Vibration Reduction in Passenger Cars,
- [12] **Sul L., Zhou H., Zhul L.** The Optimization of a Middle-sized Passenger Car Steering Wheel Vibration at Idle Speed, College of Automotive, Tongji University
- [13] **Slave R. B., Vianna E. P., Persegui O. T., Andrade F., Fonseca F., Felicio J. A., Spada J. N., Comparini F., Berti O., Zambon H.** Vibration Mode Study of Steering Columns for Commercial Vehicles, Ford Motor Company

- [14] **Chen S., Wang D., Tan G., Zan J.** Modal Analysis of Automotive Steering System Based on Finite Element Method, State Key Laboratory of Automotive Simulation and Control, Jilin University & Changan Automobile Engineering Institute
- [15] **Guo L., Ji G., Zhao L., Li J.** Static and Dynamic Finite Element Analysis on the Steering System of Automobiles, School of Mechanical Engineering and Automation & Editorial Department of Journal of Northeastern University, Northeastern University
- [16] **Xiang G., Yinxiao W.** Modal Analysis of Electronic Power Steering Based on Finite Element Method, Jiangsu University
- [17] **Bianchini E. (2005).** Active Vibration Control of Automotive Steering Wheels, SAE International
- [18] **Landreau T., Gillet V.** Analysis and Control of Vehicle Steering Wheel Angular Vibrations, Auto Chassis International, Chassis Engineering Department
- [19] **Zhang L., Dong E. (2012).** Dynamics Simulation on Vehicle Steering Mechanism, nd International Conference on Electronic & Mechanical Engineering and Information Technology (EMEIT-2012), Automotive and Transport School, Tianjin University of Technology and Education
- [20] **Othman W. B. (2011).** Experimental Study of Steering Wheel Vibration in Dynamic Condition, Bachelor of Mechanical Engineering (Automotive), Fakulti Kejuruteraan Mekanikal, Universiti Teknikal Malaysia Melaka
- [21] **Yang Jim Shin, Chirl Soo Shin (1999).** The Study for the Reduction of Idle Vibration of Steering System through the Use of a Weight Reduction Method, Hyundai Motor Co., Ltd., SAE Technical Papers
- [22] **Kim K., Choi I., Kim C. (2007).** A Study on the Advanced Technology Analysis Process of Steering System for Idle Performance, Noise and Vibration Conference and Exhibition, St. Charles, Illinois
- [23] **Abreu R. D. A., Moura F. (2012).** Operational Modal Analysis Techniques Used for Global Modes Identification of Vehicle Body Excited From a Vehicle in Idle Engine
- [24] **Britto V. A. J., Loganathan E., Sadasivam S., Hatti K., Sankaranarayana S. (2013).** Methodology of Steering Assembly Development for NVH for Medium and Heavy Commercial Vehicle, Ashok Leyland Technical Centre
- [25] **Fujiwara Y., Nakayasu M. (1971).** Analysis of Vibrational Modes of Vehicle Steering Mechanisms, Nissan Motor Co., Ltd.
- [26] **Sugita H., Asai M.** Experimental Analysis for the Steering Wheel Vibration Using Mechanical Impedance Methods, Toyota Motor Corporation
- [27] **Kim J.H., Choi S.P. (1987).** An Application of a Dual Mode Dynamic Damper to Control Steering Wheel Shimmy and Shake Problems, SAE Paper 871153, 1987-11-08

- [28] **Min F., Wen W., Zhao L., Yu X., Xu J. (2012).** Shimmy Identification Caused by Self-Excitation Components at Vehicle High Speed, Proceedings of the FISITA 2012 World Automotive Congress, Volume 13: Noise, Vibration and Harshness
- [29] **Shi W., Wu G., Wang S., Chen Z. (2012).** Improvements of Steering Wheel's Idle Shaking, Proceedings of the FISITA 2012 World Automotive Congress, Volume 13: Noise, Vibration and Harshness
- [30] **Xie R., Liu Z., Long S., Tian Z. (2012).** Test and Simulation Integrated Transfer Path Analysis and Optimization of the Steering Wheel Vibration in Idle, Proceedings of the FISITA 2012 World Automotive Congress, Volume 13: Noise, Vibration and Harshness
- [31] **Giacomin J., Shayaa M. S., Dormegnie E., Richard L.** A Frequency Weighting for the Evaluation of Steering Wheel Rotational Vibration, Dept. of Mech. Engineering, The University of Sheffield
- [32] **Ereke İ. M. (1986).** Katı Ön Aksta Yol Pürüzlülüğünün Direksiyon Sarsıntısına Etkisi, Doktora Tezi, İstanbul Teknik Üniversitesi Fen Bilimleri Enstitüsü
- [33] **Jeon H. B. (2010).** Proposed Automobile Steering Wheel Test Method for Vibration, School of Engineering and Design Brunel University
- [34] **Yoo W., Na S. and Kim M. (2011).** Relationship Between Subjective and Objective Evaluations of Steering Wheel Vibration, Journal of Mechanical Science and Technology 25 (7) 1695~1701
- [35] **Heylen W., Lammens S., Sas P. (1997).** Modal Analysis Theory and Testing, Katholieke Universiteit, Leuven
- [36] **Friswell M. I., Mottershead J. E. (1996).** Finite Element Model Updating in Structural Dynamics, Dept. of Mechanical Engineering, University of Wales Swansea, Swansea, U.K.
- [37] LMS Virtual. Lab Solutions Guide, LMS Intl., Leuven, 2006
- [38] **Shwetha G.N., Ramesh H.R., Shankapal S. R. (2013).** Modeling, simulation and implementation of a proportional-derivative controlled column-type EPS, International Journal of Enhanced Research in Science Technology & Engineering, ISSN: 2319-7463 Vol. 2 Issue 9, September-2013, pp: (10-19)
- [39] **Bennett S.** Heavy Duty Truck Systems, Fifth Edition, 2011, pg. 760-766
- [40] **Silva, A. R. C. R. da (2013).** Early Phase of the Cross Car Beam Concept Development, Faculdade de Engenharia da Universidade do Porto Mestrado Integrado em Engenharia Mecânica
- [41] **P. Holen (2006).** On modally distributed damping in heavy vehicles, Ph.D. dissertation, Vehicle Engineering, Royal Institute of Technology (KTH)
- [42] **Bagley, M.R. (2005).** Modeling an Automobile Steering System Using Axiometric Design's Design Matrix and the Design Structure Matrix, Massachusetts Institute of Technology

CURRICULUM VITAE



Name Surname: Begüm DEREBAY
Place and Date of Birth: Üsküdar / 1986
Address: Istanbul
E-Mail: begumdrby@hotmail.com
B.Sc.: Yıldız Technical University Mechanical Engineering